LAPPEENRANTA UNIVERSITY OF TECHNOLOGY
LUT School of Engineering Science
Degree Program in Chemical Engineering

Ville Puhakka

DEVELOPMENT OF NOVEL HYBRID ADSORBENTS FOR RECOVERY OF RARE EARTH ELEMENTS FROM MINING EFFLUENTS

Examiners: Prof. Mika Sillanpää
MSc. Deepika Lakshmi Ramasamy

ABSTRACT

Lappeenranta University of Technology
LUT School of Engineering Science
Degree Program in Chemical Engineering

Ville Puhakka

Development of novel hybrid adsorbents for recovery of rare earth elements from mining effluents

Master's Thesis, 2017

85 pages, 28 figures, 14 tables

Examiners: Professor Mika Sillanpää
MSc. Deepika Lakshmi Ramasamy

Keywords: Adsorption, acid mine drainage, rare earth elements, hybrid adsorbents

The main objective of the thesis was to develop novel hybrid adsorbents for the recovery of rare earth elements (REEs) from acidic mine waters. Three different groups of adsorbents, based on different combinations of backbone materials (silica-chitosan, carbon nanotubes-silica, and activated carbon-silica) were synthesized in this work. 3-aminopropyl-triethoxy-silane (APTES) and trimethoxy-methyl-silane (MTM) were utilized as coupling agents for the fabrication of chemically immobilized silica-based adsorbents whereas 1-(2-Pyridylazo)-2-naphthol (PAN) and acetylacetone (AcAc) were used for ligand modifications. The potential of these hybrid adsorbents was studied in a single component system, whole REE-series, and REE spiked real AMD (acid mine drainage) in terms of REE recovery. Among these materials, silica-chitosan hybrid gel beads proved to be the most efficient adsorbents for REE recovery from AMD as they were capable of removing an entire group of REEs almost instantly, from a solution containing significantly higher amounts of competing ions. Hence, the studies revealed that the hybrid gel beads could serve as a promising option for REE recovery applications from acidic mine waters. It was also found that the ligand modification and surface functionalization step enhanced the selectivity of adsorbents towards REEs. Moreover, 85-95 % recovery of REEs was successfully achieved with all the synthesized adsorbents when 1M HNO_3 was used for a desorption period of 5-15 minutes. Additionally, selective scandium recovery from common industrial impurities was assessed with physically adsorbed and chemically immobilized silica gels and a strategy to selectively separate scandium in the presence of iron (Fe^{3+}), aluminum (Al^{3+}) and gold (Au^{3+}) was developed.

TIIVISTELMÄ

Lappeenrannan teknillinen yliopisto
LUT School of Engineering Science
Kemiantekniikan koulutusohjelma

Ville Puhakka

Uusien hybridi-adsorbenttien kehittäminen harvinaisten maametallien poistamiseksi kaivosvesistä

Diplomityö, 2017

85 sivua, 28 kuvaa, 14 taulukkoa

Työn tarkastajat: Professori Mika Sillanpää
DI Deepika Lakshmi Ramasamy

Avainsanat: Adsorptio, happamat kaivosvedet, harvinaiset maametallit, hybridi-adsorbentit

Tämän opinnäytetyön pääasiallisena tavoitteena oli uusien hybridi-adsorbenttien kehittäminen harvinaisten maametallien (REE, *rare earth elements*) talteen ottamiseksi happamista kaivosvesistä. Tutkimuksessa vertailtiin kolmea eri materiaalien yhdistelmää adsorbenttien perustana (silika-kitosaani, hiilinanoputki-silika ja aktiivihiili-silika). Silikapohjaisten adsorbenttien kemialliseen sitomiseen käytettiin 3-aminopropyyli-trietoksi-silaania (APTES) ja trimetoksi-metyyli-silaania (MTM), kun taas adsorbenttien kelatointiin käytettiin pyridyyli-atso-naftolia (PAN) ja asetyyliasetonia (AcAc). Uusien hybridi-adsorbenttien potentiaalia tutkittiin yhden komponentin liuoksissa, koko REE-sarjalla ja happamalla kaivosvedellä, johon oli lisätty harvinaisia maametalleja. Silika-kitosaani -geelihelmet osoittautuvat tehokkaimmiksi adsorbenteiksi harvinaisten maametallien talteen ottamiseen tutkitusta kaivosvedestä. Nämä adsorbentit pystyivät poistamaan lähes välittömästi koko REE-sarjan metallit huomattavasti korkeampia pitoisuuksia kilpailevia ioneja sisältävästä kaivosvedestä. Tutkimuksen perusteella hybridi-geelihelmet vaikuttavat lupaavalta ratkaisulta harvinaisten maametallien talteen ottamiseksi happamista kaivosvesistä. Kemiallinen muokkaus yllä mainituilla yhdisteillä lisäsi adsorbenttien selektiivisyyttä harvinaisia maametalleja kohtaan. 85-95 % adsorboiduista maametalleista pystyttiin poistamaan adsorbentin pinnalta 5-15 minuutin (1M) typpihappo-uutolla. Lisäksi työssä tutkittiin skandiumin selektiivistä adsorptiota yleisiä kaivosvesissä esiintyviä kilpailevia ioneja sisältävistä liuoksista fysikaalisesti muokatuilla ja kemiallisesti sidotuilla silikageeli-adsorbenteilla. Tulosten perusteella kehitettiin suunnitelma selektiiviseen skandiumin talteenottoon rautaa (Fe^{3+}), kultaa (Au^{3+}) ja alumiinia (Al^{3+}) sisältävistä liuoksista.

Table of contents

List of Symbols 4

List of Abbreviations 5

List of figures 6

THEORY 10

1 Introduction 11

1.1 Scientific background 12

1.2 Rare earth elements chemistry 15

1.3 Adsorption 19

1.3.1 Effect of acidity 20

1.3.2 Effect of charge 21

1.3.3 Adsorption isotherms 21

1.4 Adsorbents 23

1.4.1 Silica 23

1.4.2 Chitosan 24

1.4.3 Carbon 27

1.4.4 Chelating agents 28

EXPERIMENTAL PART 31

2 Used materials 32

3 Characterization techniques 32

4 Batch adsorption experiments 33

5 Application I: Selective separation of scandium 34

5.1 Synthesis 34

5.2 Binary system 36

5.3 Multi-component system 39
5.4 Characterization 41
5.5 Adsorption mechanism 43
6 Application II: Hybrid adsorbents for recovery of REEs from AMD 44
6.1 Type I: silica-chitosan hybrid gel beads 44
6.1.1 Synthesis 44
6.1.2 Significance of modification 47
6.1.3 Intra-series REE behavior 49
6.2 Type II: carbon nanotube -nanosilica composites 52
6.2.1 Synthesis 52
6.2.2 Effect of pH 53
6.2.3 Intra-series REE behavior 54
6.3 Type III: Activated carbon -nanosilica composites 57
6.3.1 Synthesis 57
6.3.2 Effect of pH 58
6.3.3 Intraseries REE behavior 59
6.4 Real mine water experiments 60
6.4.1 Type I: silica-chitosan hybrid gel beads 62
6.4.2 Type II: carbon nanotube -nanosilica composites 65
6.4.3 Type III: activated carbon -nanosilica composites 66
6.5 Characterization 67
6.6 Comparison 71
6.6.1 Adsorption capacities 71
6.6.2 REE recovery from AMD 74
6.6.3 Adsorption mechanism 76

6.6.4 Silicon leaching 76

6.6.5 REE recovery from adsorbents 77

7 Future outlook 77

8 Conclusions 78

References 80

List of Symbols

C_e	equilibrium concentration	mg/L
C_i	initial concentration of the solution	mg/L
K_f	Freundlich affinity constant	L/mg
K_L	Langmuir affinity constant	L/mg
K_S	Sips affinity constant	L/mg
m	mass of adsorbent	mg
n_f	Freundlich heterogeneity factor	-
n_s	Sips heterogeneity factor	-
q_e	equilibrium adsorption capacity	mg/g
q_m	maximum adsorption capacity	mg/g
V	volume of the solution	L

List of Abbreviations

AcAc	Acetylacetone
AMD	Acid mine drainage
APTES	3-aminopropyl-triethoxy-silane
APTMS	3-aminopropyl-trimethoxy-silane
CIS	Commonwealth of independent states
CNT	Carbon nanotube
DTPA	Diethylene-triamine-penta-acetic acid
EDC	1-ethyl-3-(3-dimethyl-amino-propyl)-carbo-di-imide
EGTA	Ethylene-glycol-tetra-acetic acid
FTIR	Fourier transform infrared spectroscopy
HREE	Heavy rare earth element
ICP-OES	Inductively coupled plasma optical emission spectrometer
Ln^{3+}	Lanthanide
LREE	Light rare earth element
MTM	Trimethoxy-methyl-silane
MWNT	Multi walled nanotube
PAN	1-(2-Pyridylazo)-2-naphthol
REE	Rare earth element
SWNT	Single-walled nanotube
TCMS	Chloro-trimethyl-silane

List of figures

Figure 1. The structure of backbone units for chitin and chitosan monomers (Ravi Kumar, 2000). 26

Figure 2. Structures of multi- (a) and single-walled (b) carbon nanotubes (Zhao and Stoddart, 2009)..... 28

Figure 3. Molecular structures of APTES (a) and MTM (b) used for chemical immobilization of silica containing adsorbents for REE removal (Ramasamy et al., 2017b). 29

Figure 4. The molecular structure of PAN (a) and keto-form of acac (b), chelating agents used for surface modification of novel adsorbents for rare earth recovery (Ramasamy et al., 2017b). 30

Figure 5. Removal of Sc^{3+}-ions from a binary system of (a) Sc-Fe, (b) Sc-Au, and (c) Sc-Al at pH 5 by various surface functionalized silica gels. Room temperature, t=4 h. (Ramasamy et al., 2017d). 38

Figure 6. FTIR spectra of MTM-modified silica gel -adsorbents (Ramasamy et al., 2017d). 42

Figure 7. Effect of pH on the surface zeta potential of physically adsorbed and chemically functionalized silica gels (Ramasamy et al., 2017d)..... 43

Figure 8. The adsorption of Sc^{3+}-, Y^{3+}-, and La^{3+}-ions from three-component solution using PAN-modified, APTES-functionalized silica-chitosan hybrid flakes and beads. Ci=10 ppm each, room temperature, t =1 h (Ramasamy et al., 2017b). 47

Figure 9. Adsorption efficiency of group II silica-chitosan hybrid gel beads on 25 ppm La^{3+}-solution. pH 2, room temperature, t=1 h (Ramasamy et al., 2017b). 49

Figure 10. Effect of temperature on the adsorption of rare earth elements with PAN- or AcAc-modified, APTES- (4) or MTM-functionalized (6) silica-chitosan hybrid gel beads. pH 2, CREE=5 ppm each, T=45 °C, t =1 h (Ramasamy et al., 2017b). 50

Figure 11. Adsorption of the whole REE-series with PAN- or AcAc-modified, APTES- (4) or MTM-functionalized (6) silica-chitosan hybrid gel beads. pH 2, C_{REE}=10 ppm each, T=45 °C, t =1 h (Ramasamy et al., 2017b)..... 51

Figure 12. Effect of pH on adsorption of La^{3+} ions with PAN-modified, APTES-functionalized CNT-nanosilica hybrid adsorbents. C_{La}=25 ppm each, room temperature, t=24 h. 54

Figure 13. Effect of contact time and temperature on adsorption of the whole REE series with PAN-modified, APTES-functionalized SWNT-nanosilica adsorbents. pH 5, C_{REE}=5 ppm each, T= 23 °C & 45 °C, t=1 h. 55

Figure 14. Comparison of various CNT- and nanosilica-based adsorbents on the removal of the whole REE-series. pH 5, C_{REE}=5 ppm each, T=45 °C, t=1 h. 56

Figure 15. Effect of pH on adsorption of lanthanum with PAN-modified, APTES-functionalized activated carbon- and nanosilica-based adsorbents. Room temperature, t=24h, C_{La}=25 ppm. 58

Figure 16. Effect of contact time and temperature on adsorption of the whole REE series with PAN-modified, APTES-functionalized AC- and nanosilica-based adsorbents. pH 5, CREE=5 ppm each, T= room temperature & 45 °C, t =1 & 24 h 59

Figure 17. Comparison of PAN-modified, APTES-functionalized activated carbon- and nanosilica-based materials on adsorption of the whole REE-series. pH 5, C_{REE}=5 ppm each, room temperature, t =1 h. 60

Figure 18. Effect of ligand grafting on adsorption of competing ions in REE recovery from AMD with functionalized silica-chitosan hybrid gel beads. pH 5, C_{REE}=5 ppm each, T=45 °C, t =1 h (Ramasamy et al., 2017b)..... 62

Figure 19. Effect of silanization and ligand modification on the selectivity of group II silica-chitosan hybrid gel beads towards competing ions. pH 5, C_{REE}=5 ppm each, T=45 °C, t =1 h. (Ramasamy et al., 2017b). 63

Figure 20. Adsorption of REEs from AMD (720 m) with the best PAN- and AcAc-modified silica-chitosan hybrid gel bead adsorbents of different preparation methods. pH 5, C_{REE}=5 ppm each, T=45 °C, t =1 h (Ramasamy et al., 2017b)..... 64

Figure 21. Comparison of PAN-modified, APTES- (3&4) or MTM-silanized (5&6) silica-chitosan hybrid gel beads on adsorption of REEs from AMD (500 m). pH 5, C_{REE}=5 ppm each, T=45 °C, t =1 h. (Ramasamy et al., 2017b)..... 65

Figure 22. Adsorption of rare earth elements from AMD with PAN-modified, APTES-functionalized CNT- and nanosilica-based adsorbents. pH 5, C_{REE}=5 ppm each, T=45 °C, t =1 h. 66

Figure 23. Comparison of PAN-modified, APTES-functionalized activated carbon- and nanosilica-based adsorbents on the recovery of rare earth elements from AMD containing the whole REE series. pH 5, C_{REE}=5 ppm each, T=45 °C, t =1 h... 67

Figure 24. FTIR spectra of PAN-modified, APTES- (4) or MTM-functionalized (3&6) silica-chitosan hybrid gel beads before and after adsorption of rare earth elements

from acid mine drainage pH 5, C_{REE}=5 ppm each, T=45 °C, t=1 h. (Ramasamy et al., 2017b). 69

Figure 25. FTIR spectra of PAN-modified, APTES-functionalized MWNT-nanosilica hybrid adsorbent before and after adsorption of rare earth elements from acid mine drainage. pH 5, C_{REE}=5 ppm each, T=45 °C, t=1 h. 69

Figure 26. FTIR spectra of PAN-modified, APTES-functionalized AC-nanosilica hybrid adsorbent before and after adsorption of rare earth elements from acid mine drainage. pH 5, C_{REE}=5 ppm each, T=45 °C, t=1 h. 70

Figure 27. Effect of pH on the zeta potential of silica-chitosan hybrid gel beads (Ramasamy et al., 2017b). 71

Figure 28. Comparison of REE removal on AMD (720 m) with the best novel hybrid adsorbents from each application and type. pH 5, C_{REE}=5 ppm each, T=45 °C, t=1 h. 75

Table I. Atomic properties of rare earth elements (Ramasamy et al., 2017b). 16

Table II. Annual production and reserves of rare earth oxides in 2009 (Long, K et al., 2010)..... 18

Table III. Notations used for prepared silica gel -based adsorbents. 35

Table IV. Effect of pH and competing ions on adsorption of scandium from binary solutions with physically modified and chemically functionalized silica gels. Room temperature, C_i=25 ppm both, t=4 h. (Ramasamy et al., 2017d). 36

Table V. Effect of pH on adsorption of scandium with physically adsorbed, chemically functionalized silica gel adsorbents from multi-component solutions containing ions including Fe^{3+}, Au^{3+}, and Al^{3+}. Room temperature, Ci=10 ppm each, t=5 h. (Ramasamy et al., 2017d)..... 40

Table VI. The most effective surface functionalized silica gel adsorbents on selective separation of scandium from various multicomponent solutions. Ci=10 ppm each, t=4 h. (Ramasamy et al., 2017d). 41

Table VII. Notations used for prepared ligand-modified, chemically functionalized silica-chitosan hybrid gel beads (Ramasamy et al., 2017b). 46

Table VIII. Notations used for CNT-nanosilica -based hybrid adsorbents. 53

Table IX. Notations used for activated carbon- and nanosilica-based hybrid adsorbents. 57

Table X. Concentrations of competing ions in pH-adjusted AMD samples from depths of 720 m and 500 m after addition of REEs (Ramasamy et al., 2017b). 61

Table XI. Adsorption capacities of the best novel hybrid adsorbents from each group on adsorption of Sc^{3+}, La^{3+}, and Y^{3+} from single component systems. pH 5, room temperature, t=24 h. 72

Table XII. Isotherm parameters for the adsorption of Sc^{3+}, La^{3+}, and Y^{3+} from single component systems with the best carbon- and nanosilica-based adsorbents used in this study. 72

Table XIII. Adsorption capacities of PAN-modified, MTM-functionalized silica chitosan hybrid gel beads (B6P) towards 16 rare earth elements in a multicomponent system based on Freundlich isotherm model. pH 5, T=45 °C, t=1 h. 73

Table XIV. Comparison adsorption equilibrium times for adsorption of Sc^{3+}, La^{3+}, and Y^{3+} with PAN-modified, APTES-functionalized CNT- and AC-nanosilica hybrid adsorbents. pH 4, Ci=25 ppm, room temperature. 74

THEORY

1 Introduction

Rare earth elements (REEs) are a group of 17 metals: 15 lanthanides (Ln^{3+}), scandium (Sc^{3+}), and yttrium (Y^{3+}). REEs occur in trivalent form and they appear together in nature due to the similar physicochemical properties among the group. They exist as diverse proportions in various minerals which make the separation of REEs a challenging task. They are used in various high-tech applications in magnets, batteries, lightweight metal alloys and catalysts. (Long, K et al., 2010; Wall, 2013). Development in the fields of magnets, catalysts and sustainable technologies have led to an increasing demand for REEs over the years. (Wall, 2013; Xue, M, 2015). The production of one specific REE is impossible to alter without affecting the production of all other metals present (Castor, Stephen, and Hedrick, James, 2006). Hence, alternative sources of REE recovery was seen as a viable option and the search for it has grown extensively in the last decade (Roosen et al., 2016). Potential secondary sources such as industrial wastes like red mud from aluminum production can contain high amounts of REEs, especially Sc^{3+}. Currently, there is no viable method for REE recovery from red mud and no major applications for red mud utilization were reported other than utilizing it for the synthesis of low-cost adsorbents (Iakovleva and Sillanpää, 2013). (Borra *et al.*, 2015). Another alternative option of REE recovery from mine waters was also explored in the last decade owing to the necessity of stable supply and increased concern of AMD disposal on the environment. Specifically tailored adsorbents for this purpose could offer a solution for selective REE removal from mine waters. However, it is considered as a rather challenging task due to the presence of high concentrations of competing ions, such as Fe^{3+}, S^{6+}, and Al^{3+}, which could cause interference to REE adsorption (Roosen *et al.*, 2016).

In this study, functionalized hybrid adsorbents were developed to combine the benefits and unique properties of different materials for REE adsorption. These synthesized adsorbents were further evaluated to study the optimal conditions for REE adsorption. Repo *et al.* and Roosen *et al.* have reported ligand-modified silica-chitosan hybrid adsorbents which combines the properties of silica gel such as high surface area, stability, and porosity along with pH-responsive functional groups of chitosan (Repo *et al.*, 2011; Roosen *et al.*, 2016). Similarly, hybrid materials were developed in this study utilizing carbon-based materials such as activated carbon and

carbon nanotubes, due to their high surface area and their exploitation in commercial and industrial advancements (Henning and von Kienle, 2010; Rao et al., 2007). Modification with specific chelating agents was employed to increase the selectivity, along with stability and durability of hybrid materials (Airoldi and Alcântara, 1995; Jal, 2004).

This thesis is mainly focused on the development of novel adsorbents for removal of rare earth elements from mine water. Secondarily, selective separation of Sc^{3+} from solutions containing Fe^{3+}, Al^{3+}, and Au^{3+} was also studied. Various supports including silica gel, chitosan, carbon nanotubes, and activated carbon were exploited over the course of study for the same purpose. The significance of surface functionalization by means of silanizations and ligand modifications were also investigated for selective REE recovery. It must be noted that the term adsorption had been used for metal cation binding onto the surface of studied sorbents in this thesis. Difference between sorption and ion exchange can be indefinite as both phenomena can occur simultaneously with certain chelating agents (Repo, E., 2011).

The thesis starts with a brief theoretical background on this study, followed up by the experimental section with results and discussion. The theory part gives a deeper insight into the motivation behind this work and offers more specific background information on this topic of interest. Experimental part I focuses on selective scandium removal from solutions containing competing ions. Experimental part II includes the development of novel adsorbents and optimization of adsorption conditions for the ultimate application of REE recovery from mine water. Significant results from this study have been used in four different articles, of which one is already published (Ramasamy et al., 2017d) and another one is (Ramasamy et al., 2017b) currently under the review prior to publishing.

1.1 Scientific background

This study was adopted from the works of Ramasamy *et al.* and they were further exploited for the synthesis of hybrid adsorbents based on the established silica results. The authors studied the adsorption of REEs with chemically immobilized and physically adsorbed silica gels (Ramasamy et al., 2017a, 2017e, 2017c). These particular adsorbents were further assessed as a part

of thesis work to selectively remove Sc^{3+} from the solution containing competing ions. Aforementioned silica gels, along with silanes and ligands used for silica modification, were utilized in the preparation of hybrid adsorbents to further improve the properties of adsorbents. A comparison study was conducted to evaluate the adsorption capacities of the synthesized hybrid materials, the selectivity of REEs and their efficiencies to recover REEs from AMD.

Ramasamy *et al.* studied REE adsorption with various silane-functionalized silica gels. Three different silica gels modified with four different silanes were used (Ramasamy et al., 2017a). Silanes employed in this study were 3-aminopropyl-triethoxy-silane (APTES), 3-aminopropyl-trimethoxy-silane (APTMS), trimethoxy-methyl-silane (MTM) and chloro-trimethyl-silane (TMCS). Effect of particle size, pH and calcination were studied in artificial and real wastewater conditions. Silica gel type with smallest particle size, highest pore volume, and smallest surface area gave best results for REE adsorption (Ramasamy et al., 2017a) and was therefore chosen as the backbone for silica-based adsorbents in further studies. Amino group-containing silanes, APTES and APTMS, established the highest efficiency for REE removal. Optimal pH for APTES- and APTMS-modifications was found at 4-5 whereas for MTM- and TMCS-modified silica it was at pH 8. The study also stated that the calcination of these functionalized silica gels at higher temperatures (> 200 ˚C) lowered the efficiency for all adsorbents. (Ramasamy et al., 2017a).

In another work of the authors, Ramasamy *et al.* studied the effect of ligand modification for aforementioned silica gel adsorbents on REE recovery from wastewater. Studied ligands were 1-(2-Pyridylazo)-2-naphthol (PAN) and acetylacetone (AcAc) (Ramasamy et al., 2017e). Two different methods for ligand modification were compared: chemical immobilization of ligands using silanized silica gels and physical adsorption on the surface of unmodified or bare silica gels. (Ramasamy et al., 2017e). Chemically immobilized adsorbents established higher efficiency than physically adsorbed ones for all other REE ions except scandium. Generally, PAN modifications showed higher capacities with better kinetics compared to AcAc modifications. (Ramasamy et al., 2017e).

In another consecutive study, Ramasamy *et al.* investigated REE adsorption with silica gels focused on understanding the coordination and surface chemistry of PAN and AcAc immobilized onto APTES functionalized silica adsorbents. Whole REE series, excluding radioactive promethium, were studied to gain deeper insight into adsorption behavior within the REE groups: light (LREE) and heavy rare earth elements (HREE) (Ramasamy et al., 2017c). The studies showed that ligand modification step, especially with PAN, reduces silicon leaching from the adsorbents, thus providing surface stability to the materials. Adsorption of LREEs was higher at lower pHs (2-5) whereas HREE adsorption was higher at pH regime above 5. APTES-functionalized and PAN-modified silica gel established highest adsorption efficiency among the studied adsorbents. (Ramasamy et al., 2017c).

Guibal *et al.* experiments with chitosan beads serve as an inspiration for preparation of silica-chitosan hybrid beads in this study (Guibal et al., 2002). Glutaraldehyde cross-linked chitosan gel beads were prepared for the adsorption of palladium. These gel beads established very high adsorption capacity for palladium, around 300 mg/g, attainable even at pH 1.5. (Guibal *et al.*, 2002). Chitosan has high amino-content which results in protonation in acidic environment and affinity towards metal ions. These are desirable properties in case of adsorption. Especially in real mine water environment where the capability to adsorb in an acidic environment is beneficial. Gelation of chitosan beads will prevent dissolving and accelerate diffusion which can be a restricting factor in chitosan adsorption. (Guibal, E., 2005).

Roosen *et al.* prepared diethylene-triamine-penta-acetic acid (DTPA) and ethylene-glycol-tetra-acetic acid (EGTA) functionalized, 1-ethyl-3-(3-dimethyl-aminopropyl) carbo-di-imide (EDC) cross-linked silica gel-chitosan hybrid adsorbent for scandium recovery from red mud. Selective scandium removal was attainable from equimolar iron solution at low pH (1.25). Good separation of scandium from bauxite leachate was also studied with column chromatography. (Roosen *et al.*, 2016).

The motivation behind the utilization of activated carbon comes from its properties. It is widely used an adsorbent material with the highest surface area among the known adsorbents. (Bart and von Gemmingen, 2005). Tong *et al*. reported successful adsorption of lanthanum, terbium, and lutetium with tannic acid modified multi-walled carbon nanotubes at single component systems

with relatively high capacities (Tong et al., 2011). Aforementioned studies have served as a background for real mine water experiments with novel hybrid adsorbents.

1.2 Rare earth elements chemistry

REEs consist of 15 lanthanides, scandium, and yttrium. They behave very similarly to each other due to their trivalent state and similar ionic radii. However, there are small differences in ionic radii and different electron configuration enable distribution into two groups: light and heavy REEs. (Castor, Stephen, and Hedrick, James, 2006). Light earth elements (LREEs) include elements from La to Gd while elements from Er to Lu are considered as heavy earth elements (HREE) (Wall, 2013; Zepf, 2013). The division is based on the number of the electrons on the f shell. Empty, half filled, and completely filled (La, Gd and Lu respectively) configurations are considered as most stable ones. (Zepf, 2013). Yttrium has similar atomic radii as holmium and it is therefore considered as HREE as it behaves more similarly in comparison to other HREEs regardless of lighter atomic weight. Electron configurations along with ionic radii and atomic weight of REEs are presented in **Table I**.

The majority of REEs are not as rare in the earth's crust as the name implies. However, this misconception existed when the group was named in 18^{th} and 19^{th} centuries. Due to similar physical and chemical behavior among REEs, they exist together and are difficult to separate from each other. (Long, K et al., 2010). According to Wall, word 'earth' in the name of REEs refers to stable oxide forms where they were first identified. Most common REEs are more abundant than copper or lead and almost all REEs are more common than silver, radioactive promethium being the only exception. (Long, K et al., 2010; Wall, 2013).

Wall describes REEs as soft metals with a silvery color and high melting points. REEs react with most nonmetallic elements at higher temperatures and oxidize fast in moist air at room temperature. (Wall, 2013). REEs tend to bond with ionic bonds due to their structure. For all REEs (except Sc) coordination numbers higher than six are common. For Sc, coordination numbers over six don't exist. (McGill, 2000). All lanthanides belong to group 3 in the periodic table along with Sc, Y, and actinides (Zepf, 2013).

Table I. Atomic properties of rare earth elements (Ramasamy et al., 2017b).

Element		Atomic number	Atomic weight	Ionic radius	Charge	
					0	+3
Sc	Scandium	21	44.96	0.75	[Ar]4s23d1	-
Y	Yttrium	39	88.91	0.9	[Kr]5s24d1	-
La	Lanthanum	57	138.91	1.032	[Xe]5d16s2	[Xe]4f0
Ce	Cerium	58	140.12	1.01	[Xe]4f15d16s2	[Xe]4f1
Pr	Praseodymium	59	140.91	0.99	[Xe]4f36s2	[Xe]4f2
Nd	Neodymium	60	144.24	0.983	[Xe]4f46s2	[Xe]4f3
Pm	Promethium	61	145	-	[Xe]4f56s2	[Xe]4f4
Sm	Samarium	62	150.4	0.958	[Xe]4f66s2	[Xe]4f5
Eu	Europium	63	151.96	0.947	[Xe]4f76s2	[Xe]4f6
Gd	Gadolinium	64	157.25	0.938	[Xe]4f75d16s2	[Xe]4f7
Tb	Terbium	65	158.93	0.923	[Xe]4f96s2	[Xe]4f8
Dy	Dysprosium	66	162.50	0.912	[Xe]4f106s2	[Xe]4f9
Ho	Holmium	67	164.93	0.901	[Xe]4f116s2	[Xe]4f10
Er	Erbium	68	167.26	0.89	[Xe]4f126s2	[Xe]4f11
Tm	Thulium	69	168.93	0.88	[Xe]4f136s2	[Xe]4f12
Yb	Ytterbium	70	173.04	0.868	[Xe]4f146s2	[Xe]4f13
Lu	Lutetium	71	174.97	0.861	[Xe]4f145d16s2	[Xe]4f14

Electron configurations of REEs from cerium to lutetium include filling of f-orbital which results in unique properties (Wall, 2013). 4f -orbital causes different behavior because it appears closer to the nucleus than full $5s^2p^6$ -octet (Zepf, 2013). 4f -electrons are causing only weak shielding effect, which results in stronger attraction between other electrons and nucleus. This phenomenon, called lanthanide contraction, leads to decreasing radius for lanthanides with increasing atomic number and therefore also increasing atomic weight. (Wall, 2013). Sc and Y are the exceptions with Sc being the smallest while the radius of Y is closest to the one of Ho. Differences in ionic radii lead to regular changes in various properties through the series. (Castor, Stephen, and Hedrick, James, 2006). 4f-electrons shielded by $5s^2p^6$ -octet allows REEs to maintain their properties regardless of the compound they are bonded with. This makes REEs valuable due to their capability to preserve their unique magnetic properties. (McGill, 2000; Wall, 2013). All REE cations without full electron shells (Ce^{3+} - Yb^{3+}) are strongly paramagnetic. The rest (Sc^{3+}, Y^{3+}, $La^{3+,}$ and $Lu^{3+)}$ are diamagnetic (McGill, 2000).

REEs have several different applications in various fields such as high-tech applications and industry. Most significant applications at 2012 include magnets (20 %), battery- and lightweight

metal alloys (19 %), catalysts (19 %), phosphorus (7 %) and glass and ceramic industry (12 %). (Long, K et al., 2010; McGill, 2000; Wall, 2013). REEs are gaining interest in growing fields of technology as they offer applications for digital technology and improved energy efficiency. Permanent magnets are at the moment most valuable application for REEs $Nd_2Fe_{14}B$ being the strongest available material for permanent magnets. Samarium, dysprosium, and terbium are also used in permanent magnets to offer different properties. The most important application of Nd-magnets is large wind turbines. (Wall, 2013). Other important examples for REE usage in environmentally friendly technologies are electric vehicles, energy-efficient lighting, rechargeable batteries and fuel cells (McGill, 2000; Wall, 2013)

Table II represents annual production and reserves estimated in 2009 (Long, K et al., 2010). In 2009, almost all REE production takes place in China totaling 95 % of production. In that particular year, total production of rare earth oxides in the whole world accounted 126 metric tons. (Long, K et al., 2010). According to Wall (2013), the REE demand will only continue to increase. It is challenging to balance REE production and demand because REEs occur together as diverse proportions in most minerals (Castor, Stephen, and Hedrick, James, 2006). REE prices have been varying significantly during last decades because of changes in prevailing demand and use. (Castor, Stephen, and Hedrick, James, 2006; Wall, 2013). Generally, the most abundant REEs are the ones with the lowest price, however, demand can affect prices significantly. High demand for neodymium magnets has increased its price in recent years. Most expensive REEs at the moment are those, which are needed for phosphors and magnets: terbium, dysprosium, and europium. (Wall, 2013). The price of the most expensive Ln^{3+}'s was in 2015 somewhere from 500 to 1 000 US dollars per kilogram for pure metals. Cheapest REEs such as lanthanum, cerium, and yttrium can cost less than 10 US dollars for a kilogram. (Xue, M, 2015).

Sc is the most valuable of REEs. In the beginning of the year 2017, the price of 99.99 % pure scandium metal was 15,000 US dollars for a kilogram ("Mineralprices.com - The Global Source for Metals Pricing," 2017). Currently, Sc is produced only as a byproduct of other processes (Kimball, S., 2017). It has significantly smaller ionic radii and especially atomic weight compared to other REEs (Ramasamy et al., 2017c). This leads to certain unique properties that no

other material possesses. Main applications for Sc are durable, light-weight metal alloys with aluminum, and solid oxide fuel cells (Kimball, S., 2017; Roosen et al., 2016).

Table II. Annual production and reserves of rare earth oxides in 2009 (Long, K et al., 2010).

Country	Production		Reserves	
	Total [tons]	Share [%]	Total [ktons]	Share [%]
Australia	0	0	5,400	5
Brazil	650	0.5	48	0.05
China	120,000	95	36,000	36
CIS	2,500	2	19,000	19
India	2,700	2	3,100	3
Malaysia	380	0.3	30	0.03
USA	0	0	13,000	13
Others	0	0	22,000	22
Total	126,000	99.8	99,000	98.1

Consumption of REEs is rising as demand increases constantly on magnet and catalyst industries (Xue, M, 2015). In future, demand is predicted to increase rapidly as sustainable technologies are getting more and more attention (Machacek and Kalvig, 2016; Ramasamy et al., 2017c). Price for rare earth elements has been volatile as production is dominated by one country. China accounts 95 % of REEs produced worldwide. (Long, K et al., 2010). Due to above-mentioned trends, recovery of REEs from other sources is becoming an increasingly important topic. Particularly because recycling of rare earth elements is very minimal. In 2011, under 1 % of end of life products containing REEs were recycled. (Binnemans *et al.*, 2013).

Some acid mine drainage waters and waste waters can contain highly elevated concentrations of rare earth elements (Strosnider and Nairn, 2010). Separating rare earths from these waters would be highly beneficial due to high demand and China's dominance in REE market (Long, K et al., 2010). Red mud from aluminum industry is one particular example of such waste (Borra *et al.*, 2015). It has relatively high REE concentration and therefore it has great potential to be utilized as a source of valuable raw materials. Small amounts of red mud are used in cement and ceramic production but any major applications do not exist. Currently, the reason for not utilizing the red mud as a REE source is a lack of viable methods (Borra *et al.*, 2015). This topic is important to study further. REEs can be recovered along with higher concentrations of other ions from highly alkaline red mud by leaching with mineral acids. Those waste streams can

include a significant amount of REEs that can be separated with suitable adsorbents. (Roosen *et al.*, 2014).

There are various methods available for REE separation from the waste waters: precipitation, solvent extraction, ion-exchange, electrochemical methods and membranes (Sadovsky *et al.*, 2016). All of these methods are facing their own challenges. Ion exchange and membranes are expensive for treating low concentration solutions. Precipitation and electrochemical separation are inefficient and produce large volumes of sludge whereas solvent extraction requires a huge amount of solvent. (Sadovsky *et al.*, 2016).

1.3 Adsorption

Adsorption is gaining attention as a separation method for rare earth elements from aqueous solutions such as mining wastewaters (Ramasamy et al., 2017c). According to Iftekhar *et al.* researchers are considering adsorption as one of the most cost-efficient and environmentally friendly methods for rare earth recovery (Iftekhar *et al.*, 2017a). Other advantages for adsorption are ease of operation, selectivity, and simplicity of design (Iftekhar et al., 2017b; McCabe, W. et al., 1993).

Adsorption is a process where cohesive forces cause a transition of the components (adsorbates) from the liquid phase to the surface of the solid phase (adsorbent) (Srivastava and Eames, 1998). It is a widely used process for air and water purification, as well as in industries for gas production and petrochemistry (Repo, E., 2011). Usually, adsorbents are a porous material with the high surface area. This offers more area where particles can attach to. These internal pores are a favorable environment for binding to occur. (McCabe, W. et al., 1993).

The efficiency of the phenomenon is based on the difference in certain properties of adsorbates. Molecular weight, shape, and polarity are factors which have an effect on the magnitude of forces binding particles on the surface of adsorbents. Divergence in these properties causes certain particles to have a greater attraction towards binding. This creates possibilities for very selective removal of numerous substances with suitable adsorbents. (McCabe, W. et al., 1993). Adsorption can be divided into chemisorption and physisorption, based on binding mechanism. In chemisorption, covalent bonds are formed between adsorbent and adsorbate. In

physisorption, however, interaction is driven by Van der Waals forces, hydrogen bonds or hydrophobic interactions. (Repo, E., 2011; Srivastava and Eames, 1998). Adsorption phenomenon generates always heat. In chemisorption produced amount of heat is usually significantly higher compared to physisorption. Usually, adsorption process can be reversed by certain methods which often include heating of the adsorbent. This process is called desorption and it is used for recovering the adsorbate materials and for regenerating the adsorbent for further use. (Srivastava and Eames, 1998).

1.3.1 Effect of acidity

Acidity is a significant factor in adsorption process as it determines the charge of the adsorbent surface by altering the protonation of the surface groups. It also has an effect on the behavior of the solution as it affects greatly on solubility, ion speciation, and degree of ionization of adsorbate. (Repo *et al.*, 2009). According to Repo, optimal pH for chitosan-based adsorbents is lower than optimal pH for silica-based adsorbents. It was stated that higher electronegativity of chitosan matrix, compared to silicon, leads to higher adsorption efficiency in the more acidic environment. (Repo, E., 2011). Therefore silica-chitosan hybrid materials could perform at lower pH regime compared to only silica-based materials.

Guibal *et al.* (2002) studied sulfur-based ligand modification on chitosan for palladium adsorption and listed pH-dependent adsorption mechanisms that could apply in this case. At low pH, sorption occurs by ion exchange via ion pair formation due to protonation. For unprotonated groups, sorption occurs as coordination ligand exchange via nitrogen-containing ligands. For less acidic solutions sorption occurs via ion pair binding and slow ligand exchange. (Guibal *et al.*, 2002).

Depending on pH, REEs will occur either as free trivalent metal ions or hydroxyl forms (Ramasamy et al., 2017e). Some REEs can also occur in oxidation states of 2+ and 4+, but these forms are either metastable or they will reduce/oxidize into trivalent forms (McGill, 2000). In basic solutions, REEs will take the form of $Ln(OH)^{2+}$ even though other forms are also present for Y and Sc. REEs including Y, La, Eu, and Er, for example, occur in Ln^{3+} form up to pH 6 as OH-forms become dominant at pH 8 and higher. Sc behaves differently compared to other REEs as

it appears in various OH-forms. At low pH-regime Sc^{3+} is dominant form but even at pH 4 only around half of Sc occurs as pure Sc^{3+} other half being $ScOH^{2+}$. (Ramasamy et al., 2017e)

1.3.2 Effect of charge

The charge is an important parameter when considering adsorption phenomenon as particles with the certain charge will repulse particles of similar charge and attract particles with opposite charge. This will have a fundamental effect on which ions are pulled on the surface of the adsorbent. (Repo, E., 2011). Charged material attracts oppositely charged ions. Hence, these ions get attached on the surface of this material to form an oppositely charged layer, Stern layer, which will repulse ions with a similar charge. This will lead to the electrical double layer where inner layer consists of immobile particles as particles on the outer layer are mobile. (Sze *et al.*, 2003). The electrostatic potential between these layers is called zeta potential. When this potential is higher than 25 V, the system is stable. (Repo, E., 2011)

1.3.3 Adsorption isotherms

Modeling of adsorption equilibrium and kinetics is an important tool for developing and designing actual adsorption processes. (Repo, E., 2011). Adsorption isotherm describes the correlation between the concentration of adsorbate in the solution and on the surface of adsorbent after the separation process (McCabe, W. et al., 1993). Isotherms are an extremely important method for describing and understanding adsorption processes. (Kumar, 2006). The most widely used isotherms, Langmuir and Freundlich, along with their combination, Sips isotherm, were selected for the modeling of adsorption capacity (Kinniburgh, 1986; Repo, E., 2011).

Langmuir isotherm presents that adsorption occurs by formation of a uniform single layer on the outer surface of the adsorbent. After formation of this single layer, adsorption reaches equilibrium as the adsorbent surface cannot take any more particles. (Dada, A. et al., 2012). Langmuir isotherm assumes constant adsorption energy all over the adsorbent and a limited number of identical sites that can only adsorb one adsorbate each. Langmuir adsorption isotherm can be represented by the following equation

$$q_e = \frac{q_m K_L C_e}{1 - K_L C_e} \quad (1)$$

Where q_e equilibrium adsorption capacity (mg/g),

q_m maximum adsorption capacity (mg/g),

C_e equilibrium concentration (mg/L),

K_L Langmuir affinity constant (L/mg).

With large K_L values, Langmuir isotherm is strongly favorable. When K_L<1, isotherm acts practically linearly. (McCabe, W. et al., 1993). Langmuir, such as another widely used isotherm, Freundlich, is around hundred years old. Nevertheless, both models have stayed in extensive use as they have the capability to fit into a wide variety of data relatively well. (Kinniburgh, 1986). Freundlich isotherm is an empirical two-parameter model that describes multilayer adsorption on the heterogeneous surface (Repo, E., 2011). Freundlich adsorption isotherm can be expressed by the following equation

$$q_e = K_f C_e^{\frac{1}{n_f}} \quad (2)$$

Where K_f Freundlich affinity constant (L/mg),

n_f Freundlich heterogeneity factor (-).

In equation (2) term $1/n_f$ represents the strength of adsorption. $1/n_f$>1 refers to cooperative adsorption, where the adsorbed particles on the surface of adsorbent have an effect on further adsorption. A lower value for the given term indicates standard Langmuir type of adsorption.

(Dada, A. et al., 2012; Liu, 2015). Sips, or Langmuir-Freundlich, isotherm is a three-parameter model which combines the two aforementioned isotherms. It approaches Freundlich isotherm in low concentrations and Langmuir in high concentrations. (Ahmed and Dhedan, 2012). When Sips heterogeneity factor approaches n_s=1, the model represents monolayer adsorption. With divergent n_s values adsorption is assumed to behave heterogeneously. (Dada, A. et al., 2012; Repo, E., 2011). Sips isotherm can be represented by the following equation

$$q_e = \frac{q_m (K_S C_e)^{n_S}}{1-(K_S C_e)^{n_S}} \quad (3)$$

Where K_S Sips affinity constant (L/mg),

n_S Sips heterogeneity factor (-).

Nonlinear least squares regression was used to fit above-mentioned isotherms on experimental data. Nonlinear regression was executed by minimizing the sum of squared errors between experimental and calculated adsorption capacities. Solver add-in for Microsoft Excel was utilized for this purpose. There are multiple mentions in literature stating that nonlinear fitting is more accurate than linear fitting. (Kinniburgh, 1986; Repo, E., 2011), (Kumar, 2006). According to Kinniburgh (1986), the linear method is often preferred over the nonlinear due to the simplicity of the method (Kinniburgh, 1986). However, there are significant drawbacks as Langmuir isotherm can be linearized in four different ways, each of them leading to different parameter values. The major advantage of nonlinear fitting compared to linearization is the fact that nonlinear method does not assume equal error distribution, unlike linear method. (Kumar, 2006).

1.4 Adsorbents

1.4.1 Silica

Silica gel is a hydrous form of silicon dioxide which is abundant in earth's crust, being an essential component in sediments, soil, and certain minerals. Silica gel consists of silicon atoms

randomly cross-linked by oxygen atoms. These structures form micelles with silica-groups inside and silanol groups on the surface. (Bart and von Gemmingen, 2005). This leads to high porosity and surface area of silica gels (Uhrlandt, 2006). Silica gel has high adsorption capacity towards polar particles and good thermal resistance. These properties combined with the prevalence and affordable price of under 2 euros per kilogram have made silica gel one of the most important industrial adsorbent (Bart and von Gemmingen, 2005; Repo *et al.*, 2009; Uhrlandt, 2006).

Annual consumption of silica gel totaled over 150,000 tons in the beginning of 21st century. Silica gel is moderately simple to regenerate as it only requires heating up to 150 °C. In addition to adsorption, it has also other important applications in coatings, thickeners, abrasives, chromatography, and supports for catalysts. (Uhrlandt, 2006). Presence of the silanol groups on the surface offers a suitable platform for different modifications by applying different ligands on the surface of silica gel. This creates various possibilities to adjust the properties of the adsorbent (Chiron *et al.*, 2003). Common modifications for silica gel adsorbents include different silanes such as APTES used in this study. (Bart and von Gemmingen, 2005).

Silica nanoparticles have been used for heavy metal adsorption with different modifications (Mahmoud and Al-Bishri, 2011; Rezvani-Boroujeni et al., 2015; Zhang et al., 2010). It has high surface area and adsorption capacity but lacks in selectivity. However, the surface of silica nanoparticles is easily modifiable due to unsaturated surface atoms, which makes it an ideal support for different modifications. (Zhang et al., 2010).

1.4.2 Chitosan

Chitin is second most abundant natural polymer after cellulose. It appears in exoskeletons of crustaceans and insects, cartilage of mollusks, and cell walls of fungi and yeasts. Chitosan is partly deacetylated form of chitin. (Hirano, 2002). Chitosan is insoluble in water but dissolves in dilute acids unlike chitin; this is due to higher degree of deacetylation. (Ravi Kumar, 2000). Chitin polymer with deacetylation degree over 60 % is considered as chitosan (Guibal, 2004; Varma et al., 2004). The basic structures of chitin and chitosan units are presented in **Figure 1**. Chitosan is an environmentally friendly material as it is biocompatible and biodegradable non-

toxic polymer. Chitosan is produced from crab and shrimp shells obtained as a leftover from the food industry. Annual production of chitin is estimated to be about 100 billion tons. (Hirano, 2002). According to Ravi Kumar (2000), production of 1 kg of 70 % deacetylated chitosan requires 6.3 kg of hydrochloric acid, 1.8 kg of sodium hydroxide, nitrogen, and water (Ravi Kumar, 2000).

Chitosan has a variety of diverse applications in the fields of biotechnology, medicine, textiles, food industry, membranes, cosmetics, and agriculture, (Hirano, 2002) but perhaps one of the most important application is water treatment. Chitosan has several properties which make it a great adsorbent. It has highly hydrophilic, adaptive structure and capability of chelating with metal ions selectively (Ravi Kumar, 2000; Roosen et al., 2014). It can be easily modified as a polymer or by adding new functional groups chemically or physically. This makes it possible to control adsorption process by adjusting selectivity, affinity, diffusion properties etc. (Guibal, 2004). However, chitosan-based adsorbents haven't yet made their breakthrough to the industrial use. The main reasons according to Guibal, are higher cost, variability of characteristics and availability controlled by demand in the food industry. (Guibal, 2004). Nevertheless, chitosan is cheaper than activated carbon and it has several beneficial properties, which makes it competitive environmentally friendly adsorbent. (Babel, 2003).

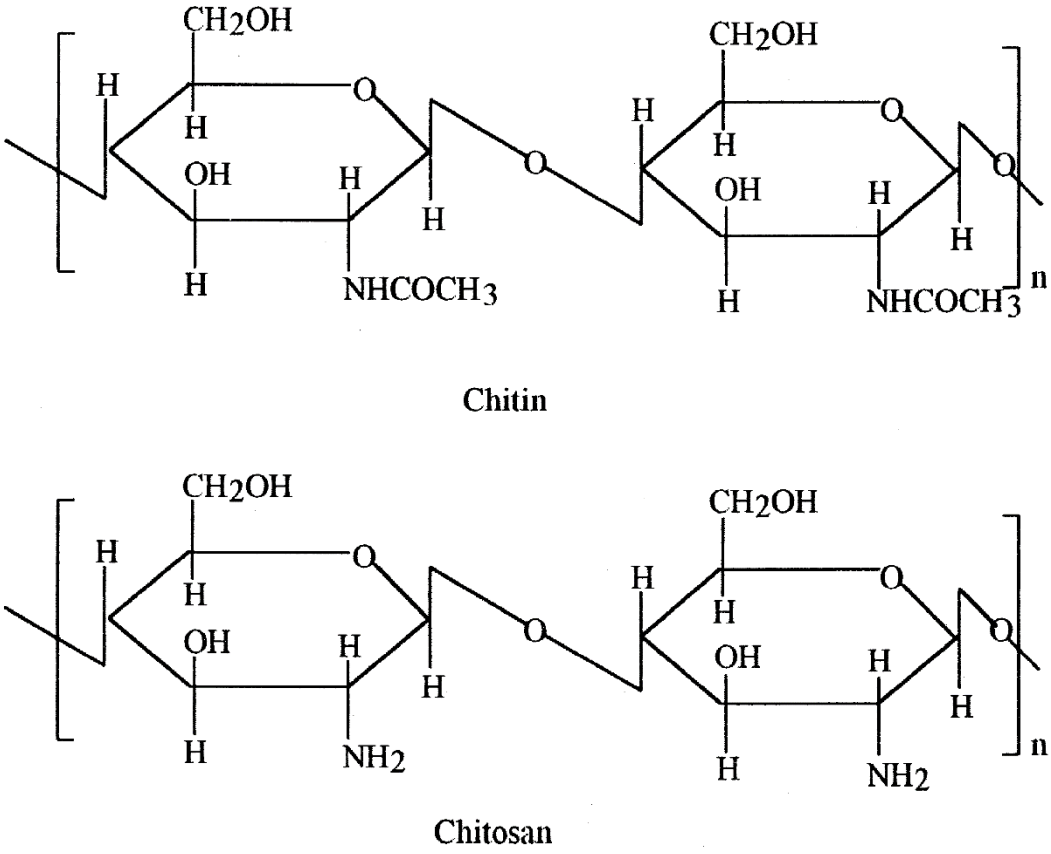

Figure 1. The structure of backbone units for chitin and chitosan monomers (Ravi Kumar, 2000).

Guibal states that degree of deacetylation and crystallinity are the most important parameters affecting the adsorption characteristics of chitosan (Guibal, 2004). Higher deacetylation state of chitin leads to increased amount of free amino groups, which are essential in adsorption of metal ions. To simplify, higher deacetylation degree leads to higher adsorption capacity (Guibal, 2004). Some amino groups in chitosan structure are not available as they are involved in hydrogen bonds. To get maximum adsorption capacity, chitosan polymer should have the maximum amount of free amino groups available for binding the adsorbate ions (Guibal, 2004). Chitosan has one of the highest chelating ability amidst natural adsorbents (Varma *et al.*, 2004). It can be also easily modified due to the high number of amine- and hydroxyl- groups and its selectivity can be controlled by immobilization of specific functional groups. (Roosen *et al.*, 2014).

1.4.3 Carbon

Activated carbon is general name describing various treated carbonaceous materials with large surface area (over 400 m^2/g up to 1500 m^2/g) and pore volume (over 0.2 mL/g). Due to these properties, its major applications are in adsorption, the most important application being water treatment. It is produced by chemical or gas activation from wood, peat, coal, or other materials containing carbon and therefore, it contains certain functional groups such as carbonyl, carboxyl, phenol, and ether groups. These surface groups are usually acidic and they can play important role in adsorption. (Henning and von Kienle, 2010).

Carbon nanotubes are nanoscale graphite sheets rolled into a tube form and closed from both heads. They can consist of only one tube (single-walled nanotubes, SWNT) or multiple parallel tubes inside each other (multi-walled nanotubes, MWNT). (Cadek *et al.*, 2010). Structures of MWNT and SWNT are presented in **Figure 2**. Carbon nanotubes (CNT) have been gaining attention as an adsorbent for metal ions and organic compounds. They have various beneficial properties for adsorbents, including stability, mechanical strength, large surface area, and surface modifiability (Tong *et al.*, 2011). CNTs possess similar surface area as activated carbon, but benefits on the uniform crystal structure. Due to their light weight, superior mechanical strength, and electronic properties CNTs have a high potential for various other applications in composites, nanoelectronics, and biosciences (Cadek et al., 2010; Khalid, P. et al., 2015). Environmental impact of carbon nanotubes needs to be studied further as various studies (Ihsanullah *et al.*, 2016; Rao *et al.*, 2007) state that raw carbon nanotubes could be harmful to the environment.

According to Rao *et al.* adsorption mechanism on CNT surface is relatively complex as it can occur via electrostatic forces, sorption-precipitation or chemical interaction via surface group attached on CNTs. They state that the acidity of CNT surface largely affects the adsorption efficiency for heavy metal ions which refer to chemisorption. (Rao *et al.*, 2007). Tong *et al.* studied the adsorption of REE ions with tannic acid modified MWNTs. This adsorbent established 4-9 mg/g adsorption for studied REEs (La, Tb, and Lu) at optimum pH of 5. (Tong *et al.*, 2011).

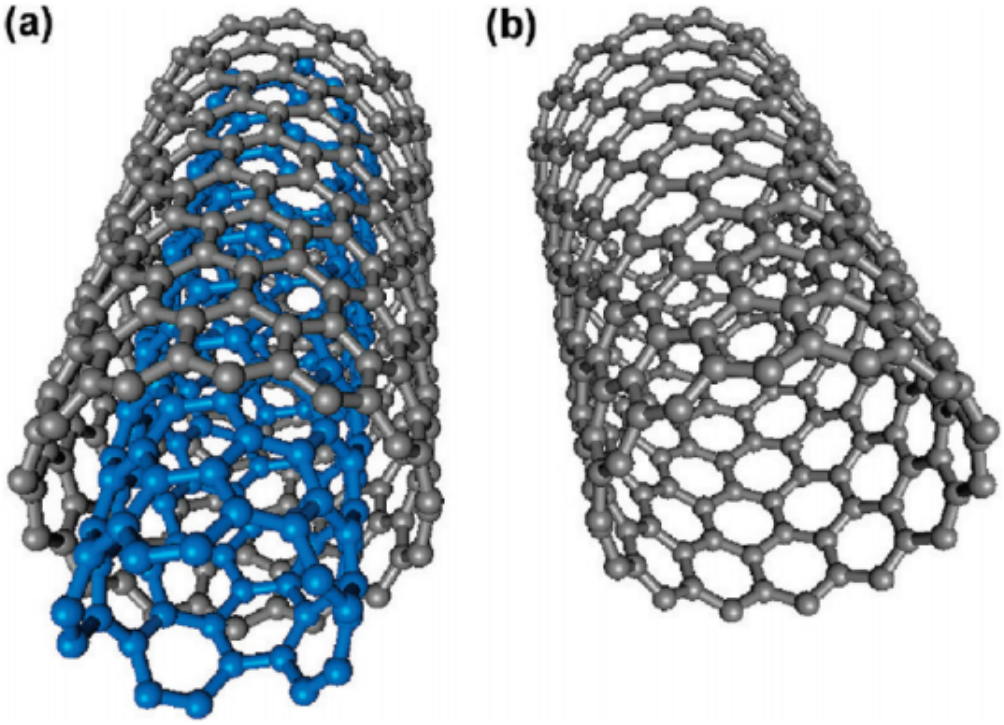

Figure 2. Structures of multi- (a) and single-walled (b) carbon nanotubes (Zhao and Stoddart, 2009).

1.4.4 Chelating agents

Specific chelating agents can be added on the surface of adsorbent to selectively adsorb certain ions from aqueous solutions. According to Airoldi and Alcantara, chelating agents usually include oxygen or nitrogen in their backbone chain. (Airoldi and Alcântara, 1995). Modification with chelating agents increases economy of the process as a smaller amount of chemicals are needed. Chelation can be executed by physical adsorption or chemical immobilization. (Ramasamy et al., 2017e). Chemicals used for functionalization of silica gel, APTES, and MTM, are presented in **Figure 3**.

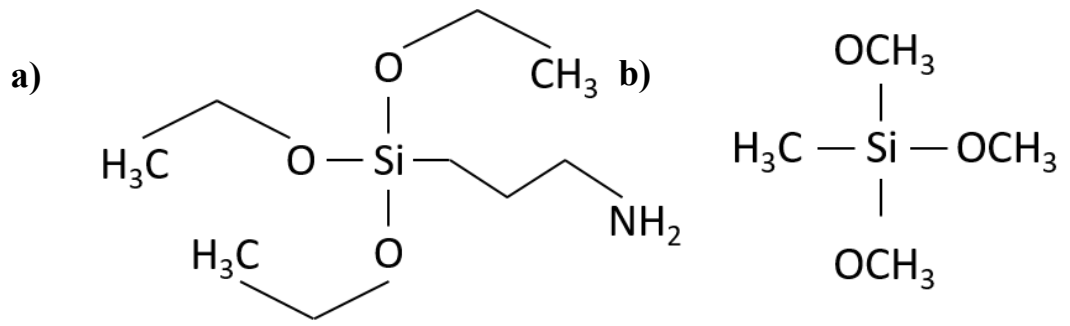

Figure 3. Molecular structures of APTES (a) and MTM (b) used for chemical immobilization of silica containing adsorbents for REE removal (Ramasamy et al., 2017b).

According to the literature that ligand modification makes silica gel more mechanically stable, immobile and insoluble to water (Jal, 2004). Unmodified chitosan can face similar challenges, being soluble in acidic conditions. Chitosan can be made barely soluble even in acidic conditions by cross-linking. (Gao *et al.*, 2000). According to the work by Jal, chemical immobilization of inorganic materials offers great possibilities to modify properties of adsorbent without losing mechanical properties of inorganic support. Silica gel has been very popular support for ligand groups due to its ease of modification, resistance for solvents and temperature, affordability, and availability. (Jal, 2004).

Chitosan polymer has naturally high nitrogen content. The free electron doublet grants ability to adsorb various metal ions. Free amino groups allow chitosan to form complexes with various metal ions (Roosen *et al.*, 2016). In acidic conditions, amino groups in chitosan are protonated. Hydroxyl- and amino groups in chitosan structure can be easily substituted by other functional groups to further modify selectivity and stability of the polymer. (Guibal *et al.*, 2002).

In this study, silica gel and chitosan adsorbents were modified with one of the two following chelating agents: PAN or AcAc to further increase their selectivity and adsorption capacity. Both ligands were earlier studied as a modification with silica, but not with chitosan (Ramasamy et al., 2017e). According to Tokalioglu *et al.*, PAN (**Figure 4a**) is a widely used chelating agent and coordination ligand for trace elements. It has a capability to form chelates in acidic and

basic pH regime via protonation of nitrogen atoms and ionization of hydroxyl groups, respectively. Metal ions can bind to pyridine- and azo-nitrogens and to oxygen atoms of hydroxyl groups. (Tokalioglu *et al.*, 2006).

Several advantages for AcAc as a ligand was mentioned in prior works. It is inexpensive, safe to use and has an ability to bind metal ions in several different ways. AcAc occurs as a mixture of tautomeric keto (**Figure 4b**) and enol forms. Both tautomers have their own characteristic way to bind metal ions. In basic pH regime, metal ions can bind to negatively charged oxygen ions. However, various binding mechanisms are possible via ring formation with oxygen atoms and π-bond formation with enol forms in neutral pHs as well. (Seco, 1989).

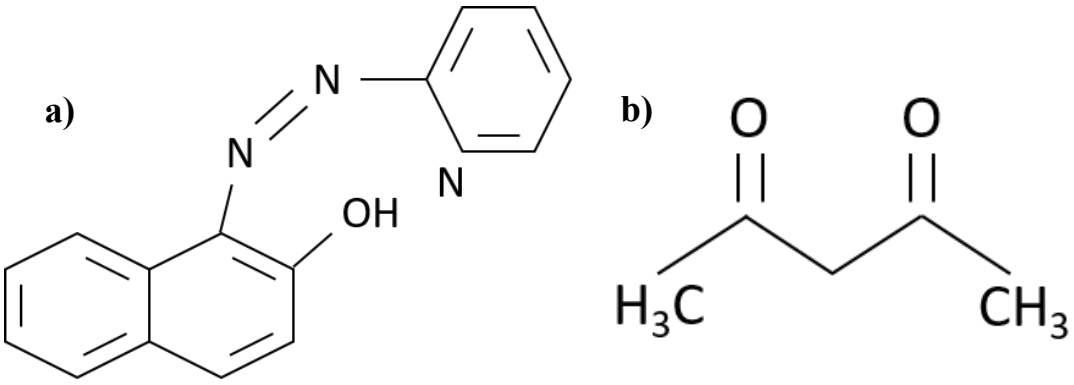

Figure 4. The molecular structure of PAN (a) and keto-form of acac (b), chelating agents used for surface modification of novel adsorbents for rare earth recovery (Ramasamy et al., 2017b).

EXPERIMENTAL PART

2 Used materials

All REE solutions used in studies (Sc^{3+}, Y^{3+}, La^{3+}, Ce^{3+}, Pr^{3+}, Nd^{3+}, Sm^{3+}, Eu^{3+}, Gd^{3+}, Tb^{3+}, Dy^{3+}, Ho^{3+}, Er^{3+}, Tm^{3+}, Yb^{3+}, and Lu^{3+}) as well as competing ions, Fe^{3+}, Au^{3+}, and Al^{3+}, were prepared from their chloride or nitrate salts provided by Sigma Aldrich. Mesoporous silica gel used in all chitosan-hybrids and silica gel-based adsorbents were provided by Merck. Pore size and particle size for aforementioned silica gel were 60 Å and 0.015 - 0.040 mm, respectively. Two different types of chitosan flakes used in this study were obtained from Sigma Aldrich. High molecular weight chitosan (C1), poly-(D-glucosamine), had a viscosity of 800 – 2,000 mPas and molar mass 310,000 – 375,000 g/mol. High viscosity chitosan from crab shells (C2), poly-(1,4-β-D-glucopyranosamine), had >400 mPas viscosity.

CNTs were obtained from Sigma Aldrich. SWNTs had >85 % carbon content (>70 % SWNT) with a particle diameter of 1.3-2.3 nm, length of >5 µm, and a surface area of 520 m^2/g. MWNTs had >90 % carbon content with 110-170 nm diameter and 5-9 µm length. Steam activated carbon pellets with the length of 0.8 mm were provided by Alfa Aesar. Silica nanopowder provided by Sigma Aldrich (>99.8 %) had a surface area of 175-225 m^2/g and a particle diameter of 12 nm.

3-aminopropyl-triethoxy-silane (APTES >98 %) was supplied by Merck whereas the other silane used for silanization of various adsorbents, tri-methoxy-methyl-silane (MTM >98 %), was obtained from Sigma Aldrich. Chelating agents, acetylacetone (AcAc >99.5 %) and 1-(2-pyridyl-azo)-2-naphthol (PAN, indicator grade) for ligand-modification of adsorbents, were provided by Sigma Aldrich. Analytical grade methanol, acetone, ethanol, and toluene were used in the synthesis of adsorbents.

3 Characterization techniques

Various instruments were used in the characterization of all adsorbents used during the study to obtain a sound understanding of the behavior of materials in the recovery of rare earths. Inductively coupled plasma optical emission spectrometer (ICP-OES), model 5110, from Agilent technologies was used for determination of initial and final concentrations from all the solutions used over the course of study. Fourier transform infrared spectroscopy (FTIR), model Vertex

70, from Bruker Optics was used to demonstrate the differences between surface chemistry of each modification. 100 scans per sample were recorded with the resolution of 4 cm^{-1} from 400 to 4000 cm^{-1}. The surface charge of adsorbents was determined as a function of pH with Malvern's Zetasizer Nano ZS.

4 Batch adsorption experiments

REE-solutions of appropriate concentration were prepared from their respective stock solution of 1000 ppm and the pH of the solutions was adjusted by 0.1 M hydrochloric acid and sodium hydroxide solutions. Inolab pH-meter (WTW series pH730) was used for pH measurements. Adsorption studies were carried out in 15 ml test tubes by adding 10 ml of suitable solution to 10 mg of adsorbent. Test tubes were then placed on the temperature controlled orbital shaker at 220 ppm for the desired time to ensure complete mixing of solution during the experiment. After the experiment, the adsorbent was removed from the solution by filtration with 25 mm polypropylene or cellulose acetate membrane syringe filter with a pore diameter of 0.2 µm. Concentrations of initial and final solutions were analyzed by means of ICP-OES instrument. Adsorption capacities were determined from the concentrations measured with ICP by using following equation

$$q_e = \frac{(C_i - C_e)}{m} V \qquad (4)$$

Where C_i initial concentration of the solution (mg/L),

m mass of adsorbent (mg),

V volume of the solution (L).

Removal percentage was calculated according to equation (5)

$$\% \text{ removal } = \frac{C_i - C_e}{C_i} \times 100\ \% \qquad (5)$$

Kinetic experiments were performed with 25 ppm single-component solutions with definite contact time interval such as 15 min, 30 min, 45 min, 1 h, 2 h, 4 h, 8 h, 16 h and 24 h. Adsorption capacities were determined with optimal contact time at concentrations of 5, 10, 25, 50, 75, 100, 150, 200, and 250 ppm. Experiments with the whole REE-series were performed with solutions containing 5 ppm of each REE unless otherwise stated.

5 Application I: Selective separation of scandium

Selective separation of Sc from artificial wastewater containing competing ions such as Fe, Au, and Al was studied with physically modified and chemically immobilized silica gel -adsorbents from earlier studies (Ramasamy et al., 2017e, 2017a, 2017c). The silica-based adsorbents (**Table III**) utilized for selective separation of scandium were used as a backbone for silica-chitosan hybrid adsorbents discussed in *6 Application II: Hybrid adsorbents for recovery of* . Adsorption of Sc was examined in binary and multicomponent solutions with competing ions to obtain further information about the selective attributes of these adsorbents.

5.1 Synthesis

Synthesis of chemically immobilized ligand-modified silica gel -adsorbents was adopted from our prior study (Ramasamy et al., 2017c). The first step in synthesis process was chemical immobilization of silica gels by letting them react in silane-toluene solution for 72 hours. Silanes used for functionalization were APTES and MTM. Ligand-modification was applied on functionalized silica gel by solvent evaporation method. Ligands used in this study were PAN and AcAc. Silica-based adsorbents prepared by these methods are presented in **Table III**. 10 V-% APTES- and MTM-solutions in toluene were used for chemical immobilization of silica gels.

Solutions were added into a closed container with silica gel in which 10 g of silica gel was mixed with 100 ml of silane-toluene solution. Reagents were stirred vigorously for 72 hours in a nitrogen atmosphere, filtrated (Ahlstrom Munktell Grade 3W filter paper) and washed with toluene, ethanol, and acetone. Finally, adsorbents were dried for 24 hours at 100 °C temperature in the oven.

Solvent evaporation was applied for dry functionalized silica gel adsorbents. 0.2 % w/w of PAN was dissolved in acetone and 1 g of AcAc was dissolved in 30 mL of methanol to prepare solutions for the solvent evaporation process. Physically adsorbed silica gels were prepared by applying above-mentioned solvent evaporation method on pure silica gel. Ramasamy *et al.* compared different ratios (1:5, 1:10 and 1:20) and concluded that 1:20 gives best results in most cases for different silica gel modifications (Ramasamy et al., 2017e). Based on these results, the ratio of 1:20 between silica gel and ligand-containing solvents were used in all methods.

Table III. Notations used for prepared silica gel -based adsorbents.

Adsorbents		Notations
Chemically immobilized Silica gel → Chemical immobilization with APTES/MTM → Ligand modification with PAN/AcAc	Silica-APTES	SE
	Silica-APTES-PAN	SEP
	Silica-APTES-AcAc	SEA
	Silica-MTM	SM
	Silica-MTM-PAN	SMP
	Silica-MTM-AcAc	SMA
Physically adsorbed Silica gel → Ligand modification with PAN/AcAc	Silica-PAN	SP
	Silica-AcAc	SA

5.2 Binary system

Selective separation of Sc from binary solutions with Fe, Au, and Al was studied at different pHs from 25 ppm (each) binary solutions. Based on preliminary experiments, studied adsorbents had a greater affinity towards Fe^{3+} ions below pH 4. Therefore pHs 4-6 are selected for further studies. Results from these experiments are presented in **Table IV**.

Table IV. Effect of pH and competing ions on adsorption of scandium from binary solutions with physically modified and chemically functionalized silica gels. Room temperature, C_i=25 ppm both, t=4 h. (Ramasamy et al., 2017d).

Adsorbent	Initial pH	Equilibrium concentration [ppm]					
		Sc-Fe		Sc-Au		Sc-Al	
		Sc^{3+}	Fe^{3+}	Sc^{3+}	Au^{3+}	Sc^{3+}	Al^{3+}
Bare Silica	**4**	22.92	6.71	23.87	18.82	23.25	20.54
	5	17.73	21.12	14.76	18.52	16.92	14.56
	6	6.19	5.46	3.76	11.79	13.57	15.25
SE	**4**	16.96	5.51	22.45	0.33	24.08	16.95
	5	6.55	10.99	6.19	1.70	20.32	15.31
	6	0.74	0.70	0.68	3.29	1.05	0.75
SEP	**4**	21.91	5.58	24.68	0.17	24.49	18.49
	5	9.38	12.83	15.70	0.22	22.65	18.40
	6	0.02	0.02	2.53	1.66	0.19	0.12
SP	**4**	21.64	4.19	24.19	18.31	23.56	20.73
	5	8.46	3.13	17.40	11.52	15.52	15.96
	6	12.79	21.46	4.18	12.12	17.14	14.46
SA	**4**	23.68	7.83	24.03	8.94	23.77	21.01
	5	9.09	10.11	18.82	4.98	15.87	15.79
	6	11.14	21.95	5.37	7.10	12.02	11.35
SM	**4**	24.47	7.82	24.21	19.65	24.65	20.29
	5	10.89	11.17	18.64	19.18	17.00	16.03
	6	18.83	23.75	5.78	13.49	21.00	17.61
SMP	**4**	24.51	7.19	24.66	14.3	24.23	20.28
	5	9.99	15.49	19.09	18.04	14.43	14.09
	6	17.91	24.05	8.01	14.54	19.58	16.69
SMA	**4**	24.14	8.24	24.17	18.86	24.29	20.34
	5	11.39	16.81	18.20	10.62	16.31	14.88
	6	17.59	23.7	7.30	15.14	20.47	17.28

Bare silica gel was capable of removing a relatively high amount of metal ions at pH 6, especially from the Sc-Fe system. However, it didn't show selectivity towards Sc^{3+} ions. SEA recorded poor adsorption of studied elements and was therefore left out from further studies. Other APTES-functionalized gels, SEP and SE, established superior adsorption capacities for studied ions but lacked in selectivity towards Sc. Physically adsorbed gels, SP and SA, resulted in the selective separation of Sc from Fe at pH 6. Both gels adsorbed more than 50 % of Sc with a negligible affinity towards Fe. However, adsorption of Al was almost equal to adsorption of Sc at all pHs. Moreover, their affinity towards Au^{3+} was very high at lower pHs. MTM-functionalized gels established highly selective removal of Sc^{3+} ions from Fe^{3+} at pH 6, even though the efficiency was lower (around 30 %). SMA had also a high affinity for Sc^{3+} over Au^{3+}, but selectivity was not as good as with Fe-solution. All MTM-modified adsorbents showed more attraction towards Al compared to Sc.

For further studies, pH 6 was selected for Sc-Fe and Sc-Au systems, whereas pH 5 was found to be optimal for Sc-Al systems. According to kinetic studies, the optimal time for Sc separation from Fe was 1 hour. After this, adsorption of both metals continued without any significant affinity towards Sc^{3+}. This could be due to the filling of Sc preferring sites on the adsorbent. For other systems, 5 hours was found to be more suitable to maximize selectivity. In Sc-Au systems, SP, SMP, and SMA established over 99 % removal of Sc with only around 8 %, 21 %, and 3 % removal of Au ions, respectively, in 5 hours. All four above-mentioned adsorbents achieved nearly complete Sc removal with 23-32 % removal of Al, SA, and SMA being the most selective ones.

Different concentration ratios of metal ions in binary solutions were utilized to further study the selectivity of modified silica gels. In addition to studies with equal parts of two cations, three different ratios were studied: 2.5:25 ppm, 25:2.5 ppm, and 25:250 ppm, with the first and second value indicating concentrations of Sc and competing ions (Fe or Al or Au), respectively. Adsorption of Sc^{3+} ions from 25:25 (Sc:Fe), 25:250 ppm (Sc: Au), 2.5:25 (Sc:Al) solution with eight types of silica gel adsorbents is presented in **Figure 5 a-c**.

As illustrated in **Figure 5a,** Sc separation from high Fe concentrations ratios was a rather challenging task for studied adsorbents, all eight adsorbents except bare silica gel established over

85 % adsorption for both components, most of them resulting over 99 % adsorption of both components. In case of bare silica gel, 60 % of Sc^{3+} was adsorbed and adsorption for Fe^{3+} was significantly lower than with other adsorbents recording just 20 %. The most selective separation of Fe^{3+} ions was achieved from equal 25 ppm solution.

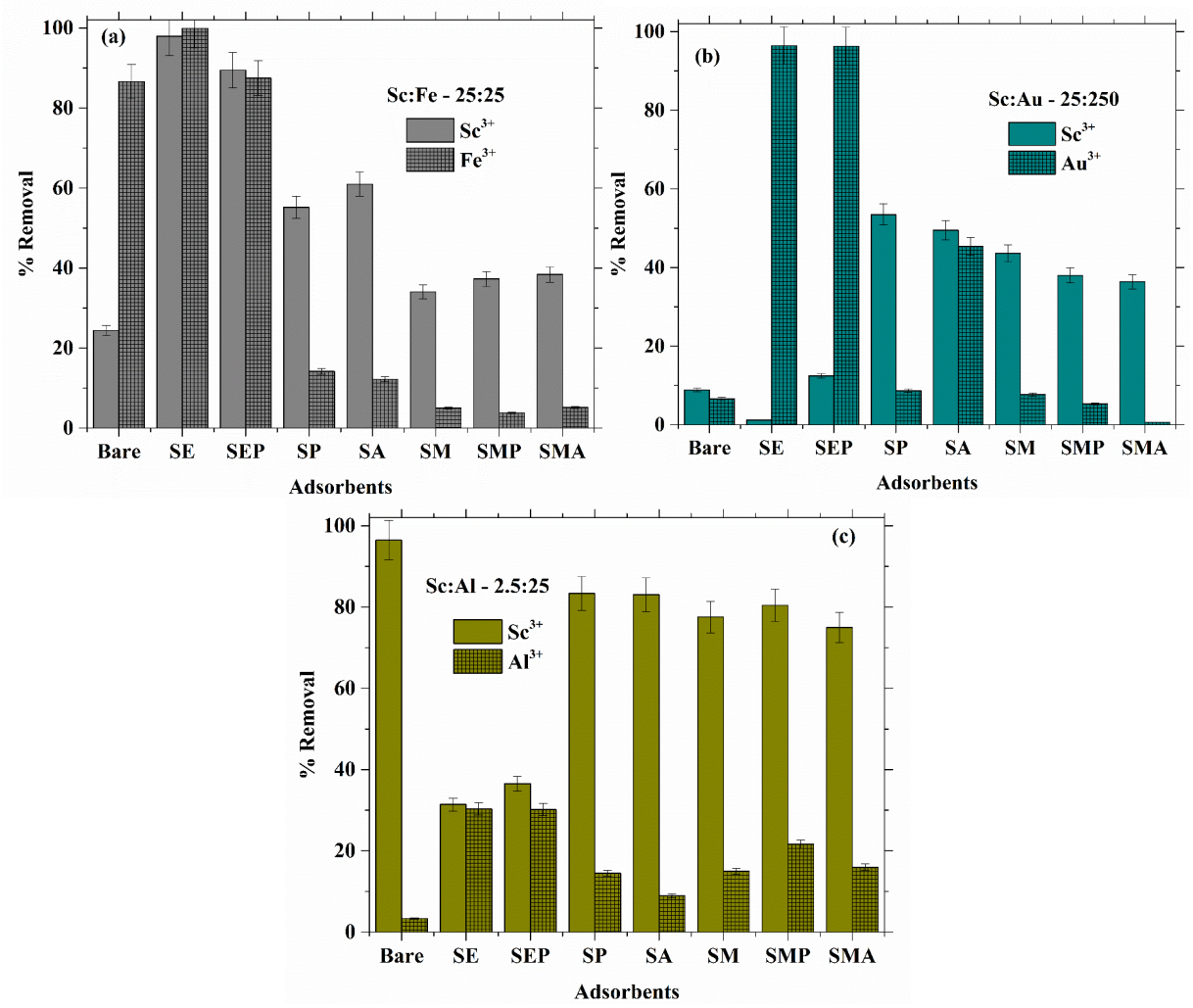

Figure 5. Removal of Sc^{3+}-ions from a binary system of (a) Sc-Fe, (b) Sc-Au, and (c) Sc-Al at pH 5 by various surface functionalized silica gels. Room temperature, t=4 h. (Ramasamy et al., 2017d).

As shown in **Figure 5b**, SMA established good selectivity towards Sc even among the 250 ppm of competing Au^{3+}-ions, as less than 1 % of Au^{3+} was adsorbed along with 10 ppm of Sc^{3+}. SP, SM, and SMP adsorbed relatively similar amounts of both ions with a slightly greater tendency towards Au^{3+} even though a number of Au^{3+} ions around the adsorbents were significantly

higher than that of Sc^{3+} ions. Nevertheless, these three adsorbents showed a rather good capability of Sc^{3+} removal from high Au concentrations. Selectivity wasn't as high at equal concentrations but affinity towards Sc was observed with SP, SM, SMP, and SMA while bare silica gel, SE, and SEP had a strong affinity for Au^{3+}. Bare silica gel along with SP showed the best performance in removal of Sc from dilute solutions (2.5 ppm of Sc^{3+} to 25 ppm of Au^{3+}).

Bare silica gel showed the best performance in removal of Sc^{3+}-ions from solutions with a higher amount of Al^{3+}-ions at concentration ratios of 2.5:25 and 25:250 ppm. At high concentration range all adsorbents, including bare silica, showed more affinity towards Al^{3+}-ions than for Sc^{3+}. From more dilute solution bare silica established over 95 % Sc^{3+} removal with only 3 % removal for Al^{3+}. Poor selectivity towards Al^{3+} was noticed at equal concentrations but SA had highest capacity for Sc^{3+} as bare silica was among the lowest ones (**Figure 5c**).

5.3 Multi-component system

Selectivity of silica gel -adsorbents towards Sc^{3+} was studied at pH range 4-6. Results are presented in **Table V** for 5 h contact time with 10 ppm initial concentration of each metal ion. SE and SEP showed again high adsorption capacity along with SA, especially at pH 6, but no selectivity towards Sc^{3+}. SMP and SMA established a greater affinity for Sc^{3+} than for other ions at pHs 5 and 6 but the difference between adsorption efficiency for Sc^{3+} and Al^{3+} was marginal. However, selective separation of Sc^{3+} from Fe^{3+} and Au^{3+} was achieved with relatively small adsorption of competing ions.

Table V. Effect of pH on adsorption of scandium with physically adsorbed, chemically functionalized silica gel adsorbents from multi-component solutions containing ions including Fe^{3+}, Au^{3+}, and Al^{3+}. Room temperature, Ci=10 ppm each, t=5 h. (Ramasamy et al., 2017d).

		Adsorption efficiency [%]			
Adsorbents	**Initial pH**	**Sc^{3+}**	**Fe^{3+}**	**Au^{3+}**	**Al^{3+}**
Bare Silica	**4**	40.86	81.75	11.95	3.41
	5	71.23	28.30	4.19	32.54
	6	74.64	56.01	7.24	69.26
SE	**4**	26.01	1.11	78.11	36.90
	5	71.78	43.63	84.52	66.27
	6	97.92	97.28	75.86	96.11
SEP	**4**	25.20	2.56	92.43	32.90
	5	55.24	14.15	86.26	47.44
	6	97.65	97.17	82.53	96.74
SP	**4**	28.80	68.25	35.27	4.70
	5	61.03	17.89	28.99	25.86
	6	79.24	60.66	32.30	76.21
SA	**4**	30.33	7.94	69.11	0.35
	5	64.06	20.82	42.61	22.05
	6	93.23	84.01	47.36	79.47
SM	**4**	17.28	72.28	55.74	2.35
	5	48.99	19.18	7.10	31.11
	6	56.23	36.51	4.94	48.53
SMP	**4**	15.30	4.32	22.96	2.35
	5	50.83	17.78	23.98	35.52
	6	44.86	6.69	14.71	32.11
SMA	**4**	13.59	29.81	1.89	1.65
	5	43.75	11.93	1.11	29.32
	6	50.63	22.90	5.33	42.95

The most feasible adsorbents for selective Sc^{3+}-removal at different conditions are presented in **Table VI**. The results are based on the multi-component experiments and could be used for selecting the suitable adsorbent for Sc^{3+}-removal depending on the ions present. MTM-functionalized adsorbents, particularly SMP and SMA, established the most selective removal of Sc^{3+} ions in presence of competitive trivalent ions. SMP achieved 45 % efficiency for Sc^{3+} with 7 %, 15 %, and 32 % removal of Fe^{3+}, Au^{3+}, and Al^{3+}, respectively. Based on these results, SMP could be utilized for Sc^{3+} separation from Fe^{3+} at optimal pH of 6. For a solution containing high concentrations of Au^{3+} ions, SMA would offer the most suitable option. At pH 5, it was established that 44 % efficiency for Sc^{3+} while adsorbing 12 %, 1 %, and 29 % of Fe^{3+}, Au^{3+}, and

Al^{3+} respectively. Both adsorbents showed superior selectivity for Sc^{3+} in a binary system with Fe^{3+} and SMA performed supremely well in high Au-concentration.

Table VI. The most effective surface functionalized silica gel adsorbents on selective separation of scandium from various multicomponent solutions. Ci=10 ppm each, t=4 h. (Ramasamy et al., 2017d).

Competing ions	Optimum pH	Effective adsorbents	Sc^{3+} removal %	Competing ions removal %	
Fe^{3+} & Au^{3+}	**5**	SM	48.99	19.18	7.10
		SMP	50.83	17.78	23.98
		SMA	43.75	11.93	1.11
	6	SMP	44.86	6.69	14.71
		SMA	50.63	22.90	5.33
Fe^{3+} & Al^{3+}	**4**	SA	30.33	7.94	0.35
Au^{3+} & Al^{3+}	**5**	Bare silica	71.2	4.19	32.54
		SM	49.0	7.1	31.1
		SMA	43.75	1.11	29.3
Fe^{3+}, Au^{3+}, & Al^{3+}	**6**	SMP	44.86	6.69	14.7 32.1

Selective separation of Sc^{3+} from Al^{3+} ions was found to be rather challenging task based on these results. Most adsorbents showed more affinity towards Sc^{3+} over Al^{3+} ions but the difference for the advantage of Sc^{3+} was relatively small. In few cases, at pH 4 (for example SM, SMP, and SMA) the adsorption of Al^{3+} ions was negligible compared to Sc^{3+} adsorption. On the other hand, at the same pH value, affinity towards Fe^{3+} or Au^{3+} was stronger than the affinity towards Sc^{3+}. Hence, from this study, it was concluded that the pH was determined to be the most influential parameter in the selective separation process, denoting pH 5 or 6 as desirable pH for Sc^{3+} separation.

5.4 Characterization

MTM-modified silica gel -adsorbents were characterized with FTIR and zeta potential analyzer to obtain deeper information about their surface modifications and adsorption mechanism. FTIR spectra for MTM-modified silica gels are presented in **Figure 6**. Other silica gel -based adsorbents used in this study were characterized for previous articles (Ramasamy et al., 2017a, 2017e, 2017c). Characteristics peaks for silica gel can be seen at 450 cm^{-1} and 800 cm^{-1} (bending and stretching vibrations of Si-O-Si respectively), 950 cm^{-1} (vibration of Si-OH), and 1100 cm^{-1}

(vibration of Si-O) (Ramasamy et al., 2017c). Peaks between 2900 cm^{-1} refer to -CH_3 and C-H structures of ligand modifications.

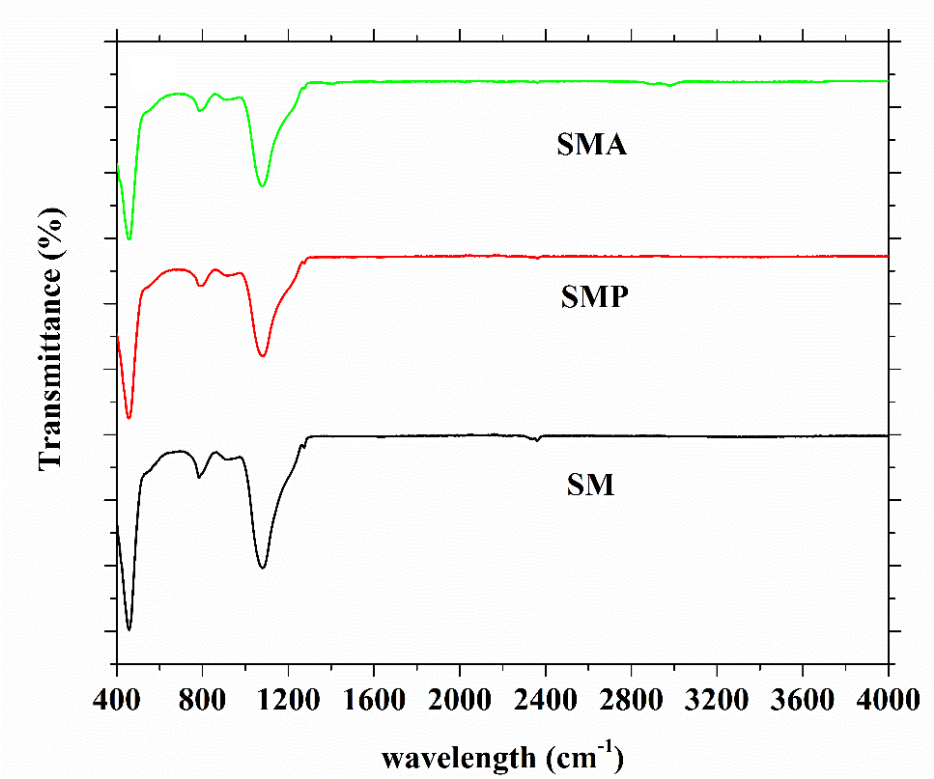

Figure 6. FTIR spectra of MTM-modified silica gel -adsorbents (Ramasamy et al., 2017d).

Effect of pH on surface zeta potential charge of MTM-functionalized and physically modified adsorbents are presented in **Figure 7**. Neutral surface zeta potential for these adsorbents was at significantly lower pH-level than for APTES-functionalized silica gels, which had isoelectric point at pHs of 7-8 (Ramasamy et al., 2017c). MTM-functionalized adsorbents had isoelectric points at pHs close to 3 and 4 (for SMP and SMA respectively) whereas physically adsorbed modifications had higher isoelectric points than their functionalized counterparts at around 4 for SP and almost 6 for SA, respectively. These results suggest that negatively charged MTM-functionalized adsorbents could attract positively charged adsorbates via electrostatic attraction forces. SA possessed relatively neutral charge at pHs 5-6. This refers to chelation via ring formation with oxygen atoms of AcAc (Seco, 1989).

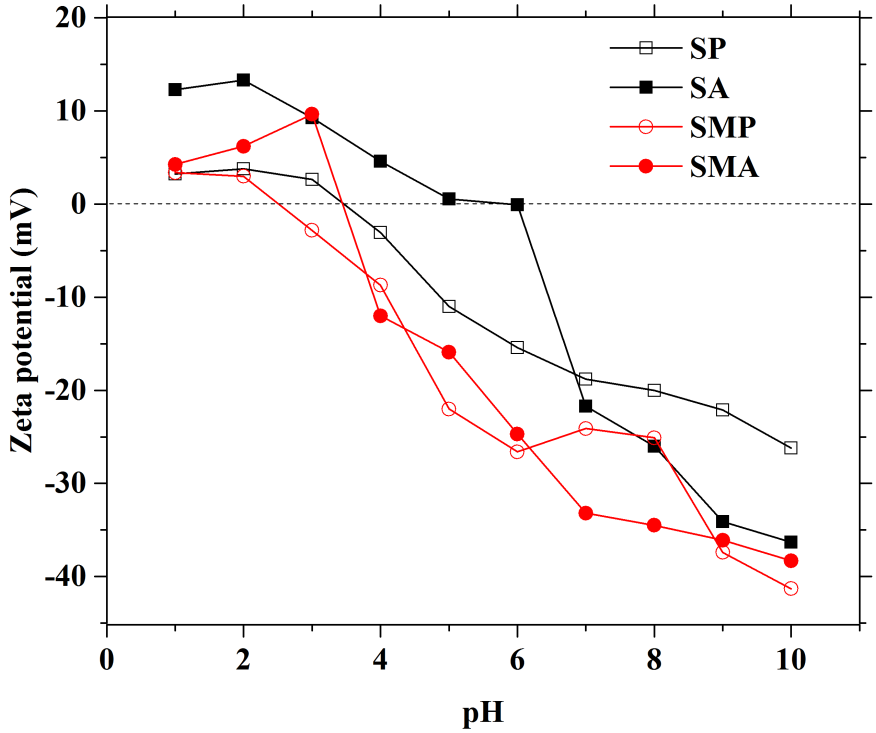

Figure 7. Effect of pH on the surface zeta potential of physically adsorbed and chemically functionalized silica gels (Ramasamy et al., 2017d).

5.5 Adsorption mechanism

Adsorption mechanism seems to be very similar to one that Ramasamy *et al.* noticed for REE adsorption with these particular adsorbents (Ramasamy et al., 2017a). MTM-functionalized adsorbents showed negative surface zeta potential over the studied pH regime and therefore attraction of metal cations could occur via electrostatic forces (Ramasamy et al., 2017a). For APTES-functionalized silica gels adsorption occurred mainly via ion-exchange as cation interacted with amino-group on APTES and hydroxyl group on silica gel. Trivalent ions could adsorb on silica gel surface via bridging with hydroxyl groups. (Hokkanen *et al.*, 2014). According to Seco, both tautomers of AcAc bind metal ions at neutral pHs via oxygen atoms by ring formation (Seco, 1989). This could partly explain the enhanced adsorption efficiency with increasing pH with a simultaneous rise in the negative surface potential of the adsorbents. PAN binds ions via free electron doublets of nitrogen atoms (Tokalioglu *et al.*, 2006) and OH-groups can contribute on adsorption at higher pH regime.

6 Application II: Hybrid adsorbents for recovery of REEs from AMD

6.1 Type I: silica-chitosan hybrid gel beads

6.1.1 Synthesis

One of the methods (Method II) of Silica-chitosan hybrid gel bead preparation was integrated from the literature (Guibal, E., 2005). The other two methods were implemented with minor adjustments on the hybridization step (Method I) or ligand grafting process (Method III). In all the methods, equal proportions of chitosan flakes and silica gel particles were mixed with 4 % (w/w) acetic acid to form a viscous solution. The resulting silica-chitosan gel was added drop by drop to 2.5 M NaOH-solution with slow stirring to form hybrid beads. Beads were left into NaOH-solution for 6 hours with until the structure was stabilized. After the stabilization, beads were washed with ultrapure water and dried in an oven at 100 °C.

As mentioned earlier, three different methods were utilized in bead preparation. These preparation methods were implemented to investigate which approach was optimal and significant for REE recovery in terms of efficiency and selectivity. Each method includes modifications varying by two different chitosan types (high molecular mass chitosan C1 and highly viscous chitosan from crab shells C2), silanes (APTES and MTM) and chelating agents (PAN and AcAc) used during the preparation. Different modifications of each bead group along with used notations are presented in **Table VII**. In the synthesis of group I beads, silica-chitosan flakes were modified with chelating agents and then dissolved in acetic acid to obtain hybrid gels which were converted to beads using method described above. Group II beads were prepared by using unmodified silica particles and chitosan flakes to prepare beads. Ligand modification was applied on the silica-chitosan hybrid wet gel beads before drying them at the 100 °C. In Method III, ligand modification was applied on the silica-chitosan acetic acid mixture. When the modification step was completed, group III beads were prepared by adding modified gel to NaOH-solution.

Solvent evaporation method used for ligand modification of silica gel above (*5.1 Synthesis*) was also applied to each hybrid bead group. 20 ml of solvent was added per one gram of silica-

chitosan flakes used for synthesis. Solvents containing PAN or AcAc were applied on unmodified silica-chitosan flakes (Method I), beads (Method II) or gel (Method III), depending on the method of preparation.

Table VII. Notations used for prepared ligand-modified, chemically functionalized silica-chitosan hybrid gel beads (Ramasamy et al., 2017b).

Adsorbents		Notations
GROUP I Silica* + chitosan + PAN/AcAc ↓ Modified flakes ↓ Beads	APTES-C1-PAN	H1P
	APTES-C2-PAN	H2P
	MTM-C1-PAN	H3P
	MTM-C2-PAN	H4P
	APTES-C1-AcAc	H1A
	APTES-C2- AcAc	H2A
	MTM-C1- AcAc	H3A
	MTM-C2- AcAc	H4A
GROUP II Silica* + chitosan ↓ Beads ↓ Modification with PAN/AcAc	Sil-C1-PAN	B1P
	Sil-C2-PAN	B2P
	APTES-C1-PAN	B3P
	APTES-C2-PAN	B4P
	MTM-C1-PAN	B5P
	MTM-C2-PAN	B6P
	Sil-C1- AcAc	B1A
	Sil-C2- AcAc	B2A
	APTES-C1- AcAc	B3A
	APTES-C2- AcAc	B4A
	MTM-C1- AcAc	B5A
	MTM-C2- AcAc	B6A
GROUP III Silica* + chitosan + PAN/AcAc ↓ Gel ↓ Beads	Sil-C1-PAN	S1P
	Sil-C2-PAN	S2P
	APTES-C1-PAN	S3P
	APTES-C2-PAN	S4P
	MTM-C1-PAN	S5P
	MTM-C2-PAN	S6P
	Sil-C1- AcAc	S1A
	Sil-C2- AcAc	S2A
	APTES-C1- AcAc	S3A
	APTES-C2- AcAc	S4A
	MTM-C1- AcAc	S5A
	MTM-C2- AcAc	S6A

*APTES/MTM-functionalized silica gel

6.1.2 Significance of modification

Ramasamy *et al.* studied REE adsorption on the silica-chitosan hybrid flakes. According to their studies, the flake form of H1P adsorbent gave best results on REE removal among all the adsorbents used over the course of study. (Ramasamy et al., 2017f). To point out the significance of gelation, H1P flakes- and beads- form were compared in terms of REE sorption efficiencies in a multi-component system. The adsorption efficiencies for Sc^{3+}, Y^{3+}, and La^{3+} ions from three component solution (10 ppm of each adsorbate) with flake form H1P at pH 2 and 4 (Ramasamy et al., 2017f) were compared to ones of H1P beads at pH 2 (**Figure 8Figure 8**).

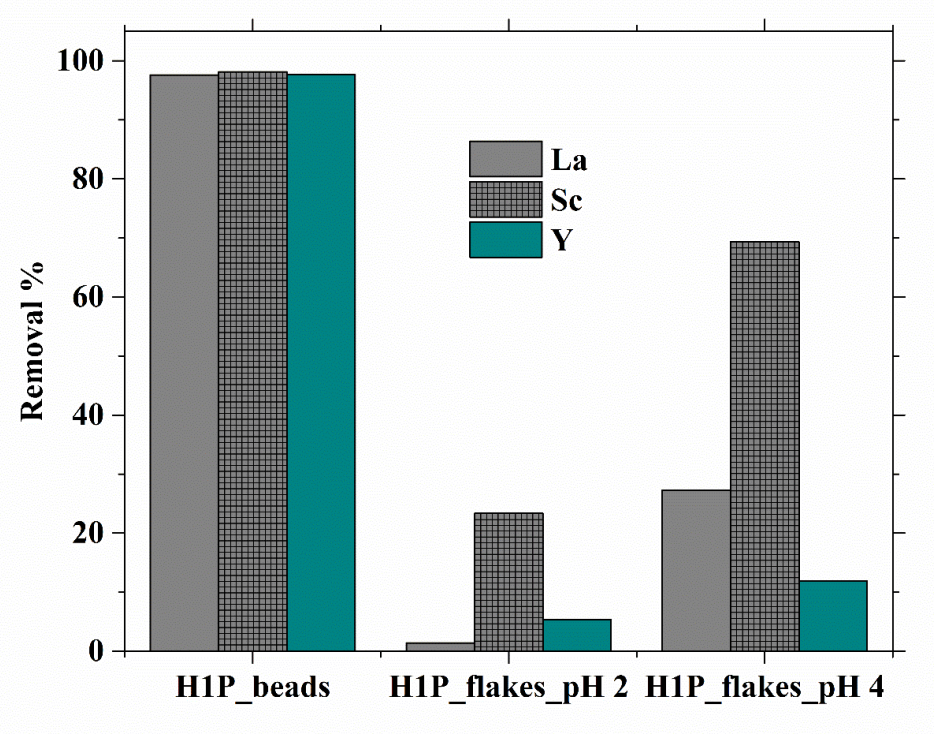

Figure 8. The adsorption of Sc^{3+}-, Y^{3+}-, and La^{3+}-ions from three-component solution using PAN-modified, APTES-functionalized silica-chitosan hybrid flakes and beads. Ci= 10 ppm each, room temperature, t =1 h (Ramasamy et al., 2017b).

Figure 8 highlights significant improvement to adsorption capacity after gelation of adsorbents. The bead form achieved over 95 % adsorption of all three elements whereas in similar conditions flake form showed very little adsorption of La^{3+} and Y^{3+} while also Sc^{3+} removal remained at barely over 20 %. (Ramasamy et al., 2017b). At pH 4, flakes were capable of considerable higher

removal percentages for Sc^{3+} and La^{3+}. On the other hand, beads were performing superbly even in the more acidic environment, at a pH value of 2. The major reasons for the notable difference could the size, low porosity, and surface area of chitosan flakes, which limits the diffusion significantly (Guibal, E., 2005; Varma et al., 2004).

The significance of hybridization can be ascertained by comparing hybrid beads to silica gel -adsorbents with a similar modification. Silica gel -adsorbents did not show notable adsorption towards REEs below pH4. (Ramasamy et al., 2017e, 2017c). Therefore, it is likely that chitosan moieties are altering the properties of hybrid adsorbent to beneficial direction. This emphasizes the contribution of protonated amine groups of chitosan in REE adsorption at low pHs. Ability to efficiently adsorb rare earths from acidic solutions could be advantageous in the treatment of mine waters. Even though adsorption at pH 2 gave very promising results, adsorption at pH 1 was unsuccessful, probably due to the notably higher amount of H^+ competing for adsorption sites. The significance of ligand modification with PAN or AcAc was evidently emphasized in real water applications in terms of selectivity and adsorption capacity. Therefore, this topic is discussed further in chapter *6.4 Real mine* water *experiments*.

Characteristics of chitosan flakes had a great impact on adsorption efficiency. For group II beads high viscosity chitosan (C2) demonstrated better results compared to high molecular weight chitosan (C1) in most conditions. Adsorption efficiencies of group II beads on 25 ppm La^{3+}-solution at pH 2 is presented in **Figure 9**. Immense difference in adsorption of La^{3+} ions could be noticed between C1 and C2 chitosan-based adsorbents as C2-based adsorbents recorded over 90 % removal of La^{3+} ions in comparison to under 40 % removal with the best C1-based adsorbent.

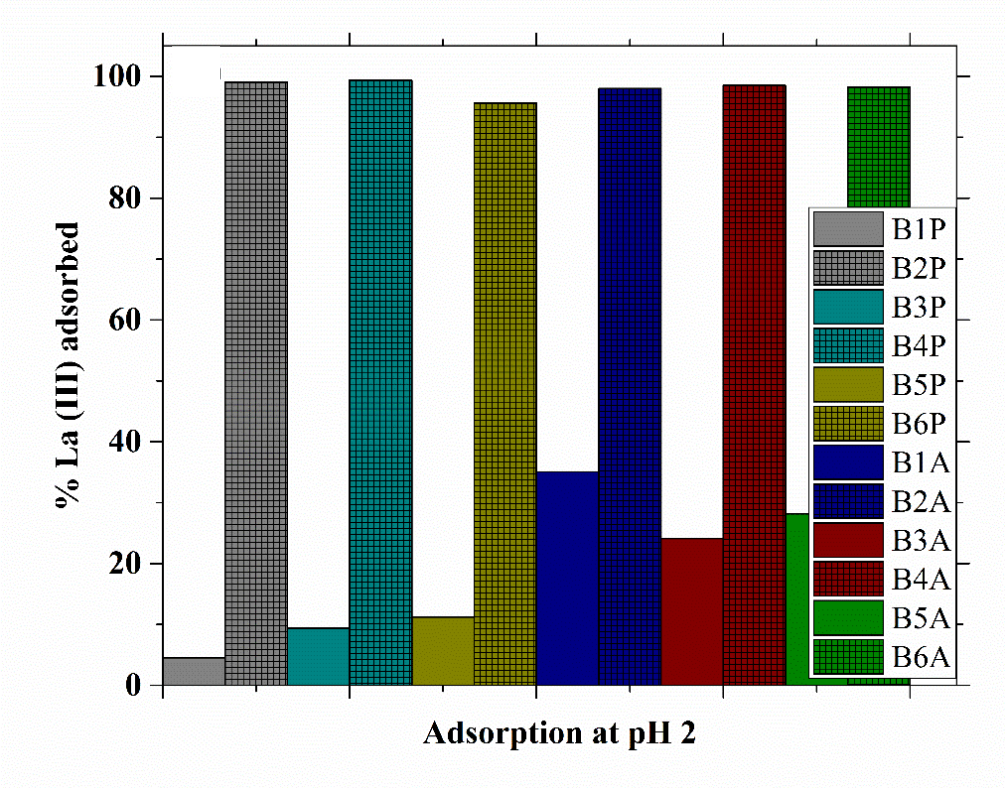

Figure 9. Adsorption efficiency of group II silica-chitosan hybrid gel beads on 25 ppm La^{3+}-solution. pH 2, room temperature, t=1 h (Ramasamy et al., 2017b).

6.1.3 Intra-series REE behavior

Ramasamy *et al.* noticed during their studies that higher temperature resulted in higher REE adsorption for silica gel -based adsorbents with same modifications. For their adsorbents, change in temperature from 23 to 45 °C increased adsorption for all the REEs but the change was seen drastically bigger for HREEs. (Ramasamy et al., 2017c). This could be due to increased mobility of ions and smaller ionic radii for heavy REEs. To gain further knowledge about the adsorption behavior and efficiency with hybrid gel beads, adsorption of the whole REE-series were investigated (**Figure 10**).

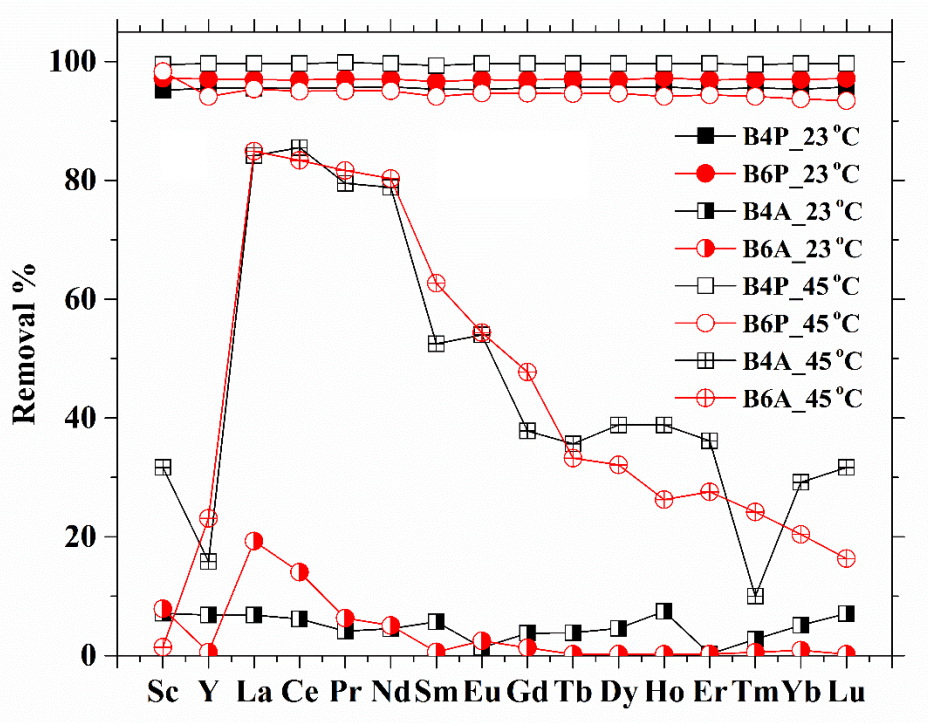

Figure 10. Effect of temperature on the adsorption of rare earth elements with PAN- or AcAc-modified, APTES- (4) or MTM-functionalized (6) silica-chitosan hybrid gel beads. pH 2, CREE=5 ppm each, T=45 °C, t =1 h (Ramasamy et al., 2017b).

Group II beads, especially B4P and B6P along with H3P from the group I stood out from a lot with their high adsorption capacity towards whole REE series. They reached nearly complete adsorption of all 16 REEs studied even at the room temperature. The rest of the group I and group III adsorbents didn't show comparable results in terms of adsorption performance. Minor increase in adsorption was observed at with an increase in temperature but it was insignificant compared to the performance of above-mentioned adsorbents. It is notable that from the group I adsorbents, C1-based adsorbent stood out, whereas for group II beads C2 backbone was more favorable.

A distinct trend towards the LREEs or HREEs was not observed for the majority of adsorbents, with B4A and B6A deviating from the group. In contrast to the behavior of silica gel -based

adsorbents (Ramasamy et al., 2017c), B4A and B6A had high selectivity towards LREEs, especially ones with largest ionic radii La^{3+}, Ce^{3+}, Pr^{3+}, and Nd^{3+}. This refers to the significance of pH on REE adsorption as adsorption of LREEs is favorable at lower pH whereas HREEs are favored at higher pH regime (Ramasamy et al., 2017c). Due to high adsorption capacity of group II beads, experiments with the whole REE-series was performed with higher REE concentrations. Adsorption of the whole REE-series at an initial concentration of 10 ppm (of each REE) is presented in **Figure 11**.

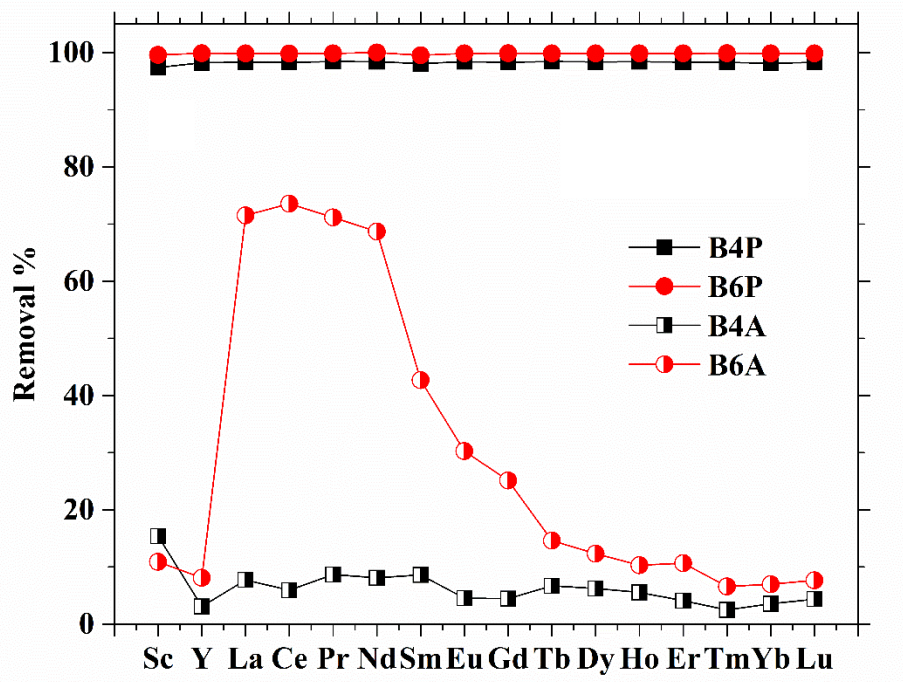

Figure 11. Adsorption of the whole REE-series with PAN- or AcAc-modified, APTES- (4) or MTM-functionalized (6) silica-chitosan hybrid gel beads. pH 2, C_{REE}=10 ppm each, T=45 °C, t =1 h (Ramasamy et al., 2017b).

When the concentration of all REEs was increased from 5 ppm to 10 ppm, the performance of B4A dropped (**Figure 11**). B6A showed even higher selectivity towards LREE group, as mentioned above. This is probably due to increased amount of these favored ions competing on suitable sites. Selectivity of B6A could lead to potential applications on selective LREE removal in acidic conditions. B4P and B6P accomplished nearly complete adsorption of all 16 REEs even at an increased concentration of 10 ppm each. Based on these results, it can be stated that

PAN-modification results in drastically higher efficiency whereas AcAc modification offers great selectivity towards intraseries.

6.2 Type II: carbon nanotube -nanosilica composites

6.2.1 Synthesis

Four different hybrid adsorbents were synthesized using silica nanoparticles and single- and multi-walled carbon nanotubes. Chemical immobilization with APTES and ligand modification with PAN was applied on these hybrid adsorbents to further increase their efficiency and selectivity. Single-walled or multi-walled carbon nanotubes were mixed with nano-silica particles in APTES-toluene -solution for 24 hours with vigorous shaking. After functionalization, adsorbents were separated from the solution by filtration (Ahlstrom Munktell Grade 3W filter paper) and washed with toluene, methanol, and ethanol prior to drying in an oven at 100 °C for 24 hours. After drying, agglomerated adsorbents were grounded in tube mill (IKA Mills, Tube Mill control) with 10 000 rpm to obtain powder-like material.

To prepare these adsorbents, carbon nanotubes and silica nanoparticles were mixed in a ratio of 1:10. 100 ml toluene-solution containing 10 V-% of APTES was used per gram of nanosilica in hybrid adsorbents. Ligand modification was applied by using two different methods. In the method I, PAN was mixed with toluene-solution prior to reaction. In method II, PAN-modification was executed with solvent evaporation method for dried hybridized materials in a manner described earlier. 0.4 % w/w PAN in toluene or acetone was used in these methods. Same methods were applied for preparation of non-hybrid adsorbents from nanosilica and different carbon nanotubes to exploit the effect of hybridization process. All prepared modifications of nanosilica and CNT-based adsorbents are presented in Virhe. Kirjanmerkin viittaus itseensä ei kelpaa..

Table VIII. Notations used for CNT-nanosilica -based hybrid adsorbents.

Adsorbent		Notation
GROUP I SWNT/MWNT-nanosilica or pure SWNT/MWNT ↓ APTES-functionalization* & PAN-modification in toluene	SWNT-Nanosilica-APTES-PAN	1SWNTsilP
	MWNT-Nanosilica-APTES-PAN	1MWNTsilP
	SWNT-PAN	1SWNTP
	MWNT-PAN	1MWP
GROUP II SWNT/MWNT + nanosilica ↓ APTES-functionalization* in toluene ↓ PAN modification via solvent evaporation	SWNT-Nanosilica-APTES-PAN	2SWNTsilP
	MWNT-Nanosilica-APTES-PAN	2MWNTsilP
	SWNT-PAN	2SWNTP
	MWNT-PAN	2MWNTP
GROUP III SWNT/MWNT + nanosilica ↓ APTES-functionalization in toluene	SWNT-Nanosilica-APTES	SWNTsil
	MWNT-Nanosilica-APTES	MWNTsil

*Only for nanosilica-containing adsorbents

6.2.2 Effect of pH

Optimal pH for REE adsorption was examined with single element adsorption experiments using Sc^{3+}, La^{3+}, and Y^{3+} ions concentration of 25 ppm with 24-hour contact time for each adsorbent. Adsorption capacities and effect of contact time are presented in chapter *6.6* Comparison. Effect of pH on adsorption of La^{3+}-ions is presented in **Figure 12**.

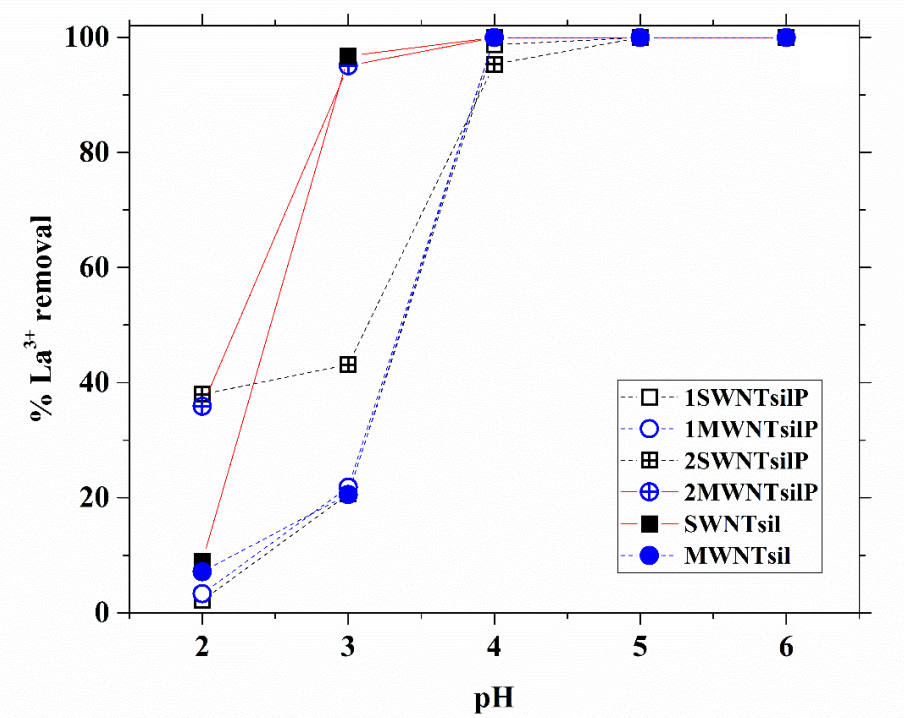

Figure 12. Effect of pH on adsorption of La^{3+} ions with PAN-modified, APTES-functionalized CNT-nanosilica hybrid adsorbents. C_{La}=25 ppm each, room temperature, t=24 h.

Trends were very similar with all three elements studied. 2SWNTSsilP and 2MWNTsilP were capable for around 40 % adsorption even at the pH 2, but the majority of adsorbents reached the maximum capacity of over 90 % adsorption only at pH 4. 2MWNTsilP and SWNTsil were capable of 90 % efficiency at pH 3 but a slight increase was still observed to pH 4. These results are in line with Tong *et al.* studies with La^{3+} as they observed similar adsorption behavior with tannic acid modified MWNT. (Tong *et al.*, 2011). At lower pH regime, competition with H^{+}-ions could be the reason for lower adsorption efficiency.

6.2.3 Intra-series REE behavior

The whole REE-series were studied to gain further understanding of CNT-nanosilica adsorbents' selective affinities and efficiencies. Also, the significance of ligand modification, CNT-structure, and preparation methods was investigated. **Figure 13** represents adsorption efficiency of SWNT-based adsorbents towards the whole REE-series at pH 5 since optimum pH for the single component system didn't show desired results for the multicomponent system.

Nonhybrid SWNT- and MWNT-adsorbents were left out of comparison due to negligible REE adsorption in all studied conditions. Nonhybrid nanosilica-modifications are discussed in chapter *6.3 Type III: Activated carbon -nanosilica* along with AC-based materials.

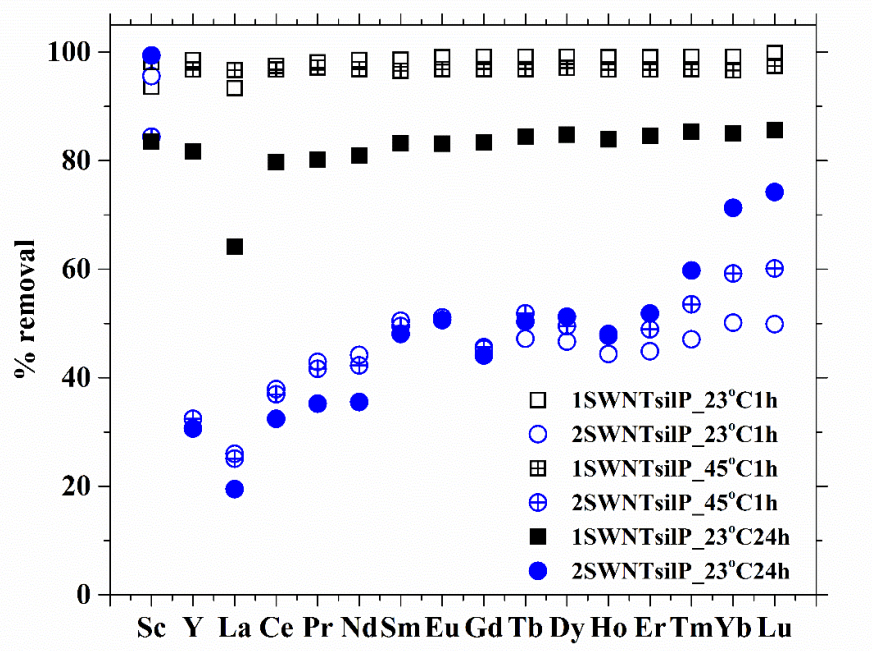

Figure 13. Effect of contact time and temperature on adsorption of the whole REE series with PAN-modified, APTES-functionalized SWNT-nanosilica adsorbents. pH 5, C_{REE}=5 ppm each, T= 23 °C & 45 °C, t=1 h.

1SWNTsilP showed almost 100 % adsorption for all REEs in both, room temperature and 45 °C, with a contact time of one hour. After 24 hours, the achieved efficiency was dropped to 80 % which suggests that after the equilibrium is reached, some desorption of REEs occurs. In all of these conditions, Method I adsorbents established considerably higher efficiencies compared to method II -adsorbents. Method II SWNT-based adsorbents showed rather similar efficiencies in all studied conditions. Increase in temperature increased adsorption of HREEs (Tm, Yb, Lu) which is in line with earlier findings (Ramasamy et al., 2017c). They observed a significant increase in temperature which shifted the affinities of modified silica gel adsorbents (studied also in *5 Application I: Selective separation of scandium*) significantly towards HREEs (Ramasamy et al., 2017c). Even higher affinities towards REEs can be observed with 24 h of process

time. All studied adsorbents established high Sc^{3+} adsorption regardless of conditions. Performance of SWNT- and MWNT-based adsorbents of two different preparation methods were compared to their counterparts without PAN-modification in **Figure 14**.

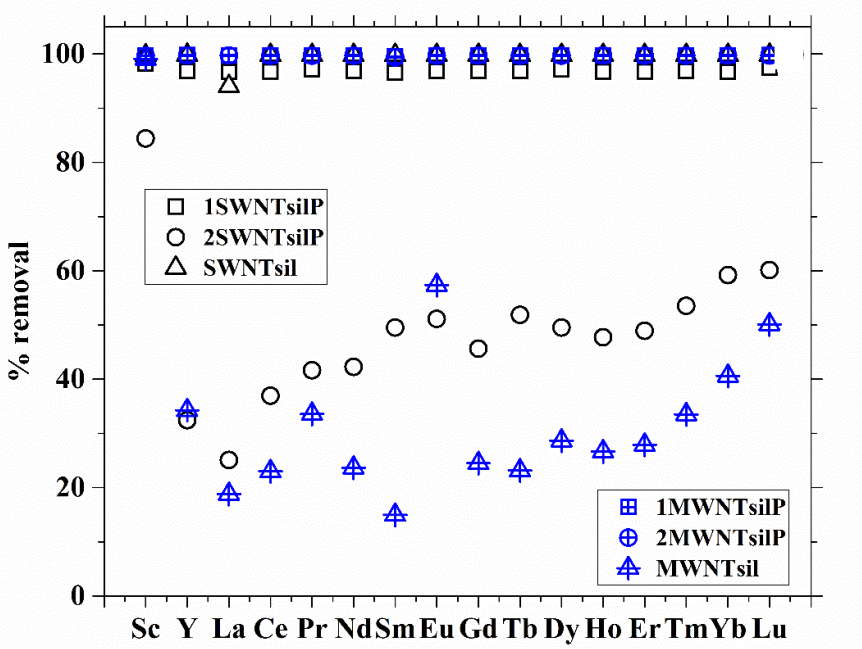

Figure 14. Comparison of various CNT- and nanosilica-based adsorbents on the removal of the whole REE-series. pH 5, C_{REE}=5 ppm each, T=45 °C, t=1 h.

Preparation method seemed to affect differently among SWNT-adsorbents and MWNT-adsorbents. PAN-modified MWNT-adsorbents showed over 95 % efficiency for all REEs whereas unmodified version established similar efficiency only for Sc^{3+} while removal of other REEs stayed significantly lower. This clearly states for the significance of ligand modification in MWNTs. Similar behavior was not observed with SWNT-adsorbents. In brief, PAN grafting onto SWNT as per Method II resulted in poor REE adsorption whereas similar modification with MWNT recorded supreme adsorption of REEs. On the other hand, PAN grafting as per Method I and no ligand grafting as per Method III on SWNTs documented excellent REE removal efficiencies whereas similar modification with MWNTs yielded poor outcome. Such contrast behavior of SWNTs and MWNTs was noticed with the different methods of preparation.

6.3 Type III: Activated carbon -nanosilica composites

6.3.1 Synthesis

Activated carbon (AC) pellets were used to prepare nanosilica-carbon hybrid adsorbents in the very similar process as described above for CNT-based adsorbents. Different modifications of AC-nanosilica adsorbents along with used notations are presented in **Table IX.**

Table IX. Notations used for activated carbon- and nanosilica-based hybrid adsorbents.

Adsorbent		Notation
GROUP I AC and/or nanosilica ↓ APTES-functionalization & PAN-modification in toluene	AC-Nanosilica-APTES-PAN	1ACsilP
	Nanosilica-APTES-PAN	1silP
	AC-PAN	1ACP
GROUP II AC + nanosilica ↓ Modified powder ↓ PAN-modification via solvent evaporation	AC-Nanosilica-APTES-PAN	2ACsilP
	Nanosilica-APTES-PAN	2silP
	AC-PAN	2ACP
GROUP III AC + nanosilica or pure nanosilica ↓ APTES-functionalization in toluene	AC-Nanosilica-APTES	ACsil
	Nanosilica-AP-TES	Nano-sil

The major difference compared to the synthesis of CNT-nanosilica adsorbents was the proportion of silica and carbon particles in the hybrid adsorbent. Activated carbon was mixed with silica nanoparticles in equal proportions. 100 ml of same silane-toluene solution was used

per 1 gram of silica in the hybrid adsorbent. Both ligand modification methods used for CNT-based adsorbents were applied onto AC hybrid adsorbents. In a similar manner, non-hybrid version of activated carbon -adsorbents was synthesized.

6.3.2 Effect of pH

Single element solutions with Sc^{3+}, La^{3+}, and Y^{3+} were utilized for pH, adsorption isotherm and kinetic studies, the latter ones are further discussed in chapter *6.6* Comparison. Effect of pH on La^{3+}-adsorption from 25 ppm solution is presented in **Figure 15**.

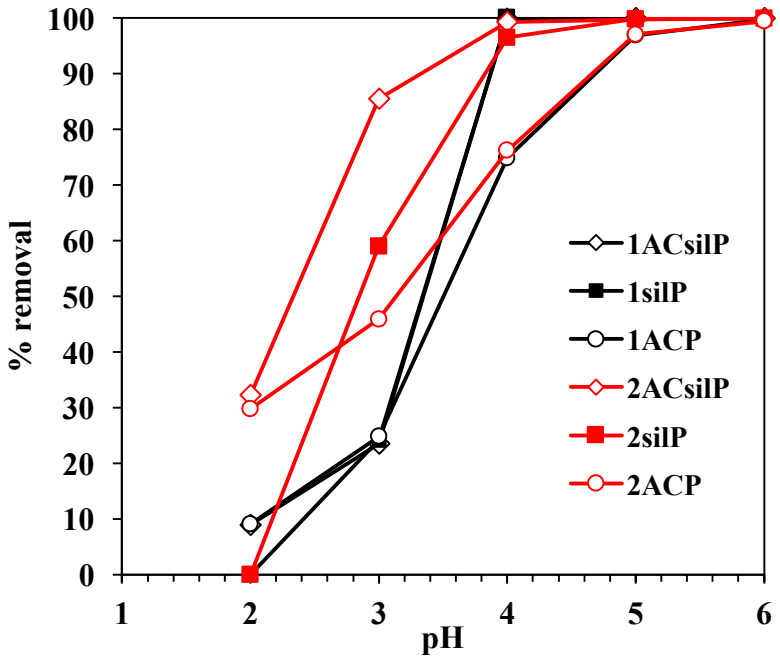

Figure 15. Effect of pH on adsorption of lanthanum with PAN-modified, APTES-functionalized activated carbon- and nanosilica-based adsorbents. Room temperature, t=24h, C_{La}=25 ppm.

All hybrid and nanosilica-based adsorbents reached over 95 % adsorption of studied ions at pH 4, the only exception being 1ACsilP for Sc^{3+} (>80 %). AC-based adsorbents without nanosilica achieved maximum removal at pH 5-6 with significantly lower efficiencies towards Y^{3+} compared to other adsorbents. Results from pH studies with AC- and CNT-hybrid adsorbents highlight the role of APTES-modified nanosilica in REE adsorption at lower pHs.

6.3.3 Intraseries REE behavior

Adsorption performance of type III -adsorbents for the whole REE series was studied to compare the differences of used modifications and gain information about affinities towards REEs. Effect of temperature and contact time for AC-nanosilica adsorbents with different ligand modification methods were compared for adsorption of the REE series, the results of which are presented in **Figure 16**.

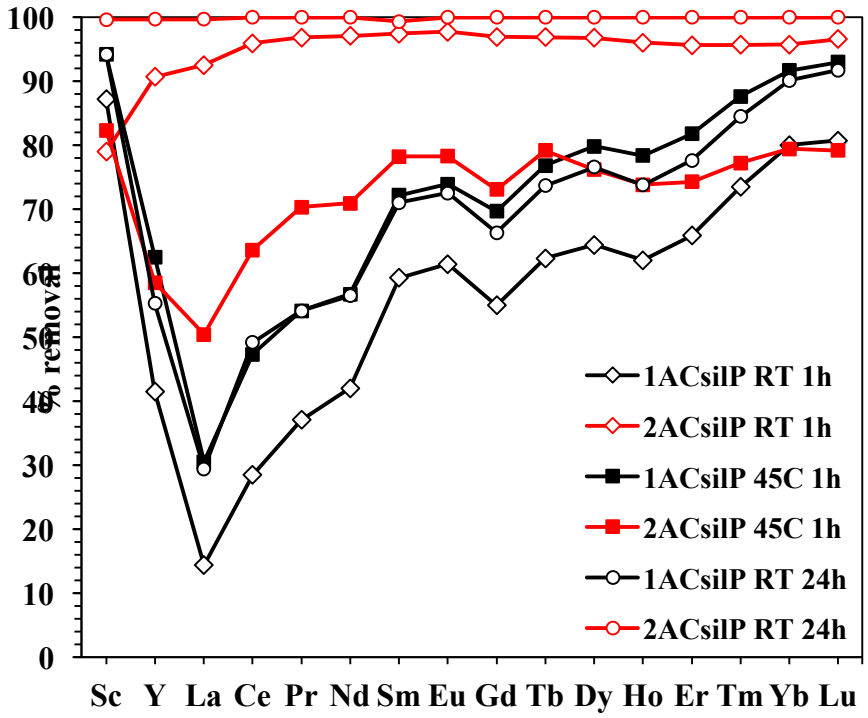

Figure 16. Effect of contact time and temperature on adsorption of the whole REE series with PAN-modified, APTES-functionalized AC- and nanosilica-based adsorbents. pH 5, CREE=5 ppm each, T= room temperature & 45 °C, t =1 & 24 h

Solvent evaporation method proved to be superior for ligand modification with application II -adsorbents. Increase in temperature seemed to affect negatively on REE adsorption for 2ACsilP, showing traces of desorption over time, in contrast to the behavior observed for the other adsorbents. However, at room temperature, 2ACsilP established superior adsorption over other studied adsorbents. REE adsorption followed a similar pattern as observed above for whole REE-series at pH around 5. The affinity towards HREEs was considerably higher than for the LREEs.

The performance of different modification on the whole REE-series was compared in **Figure 17**.

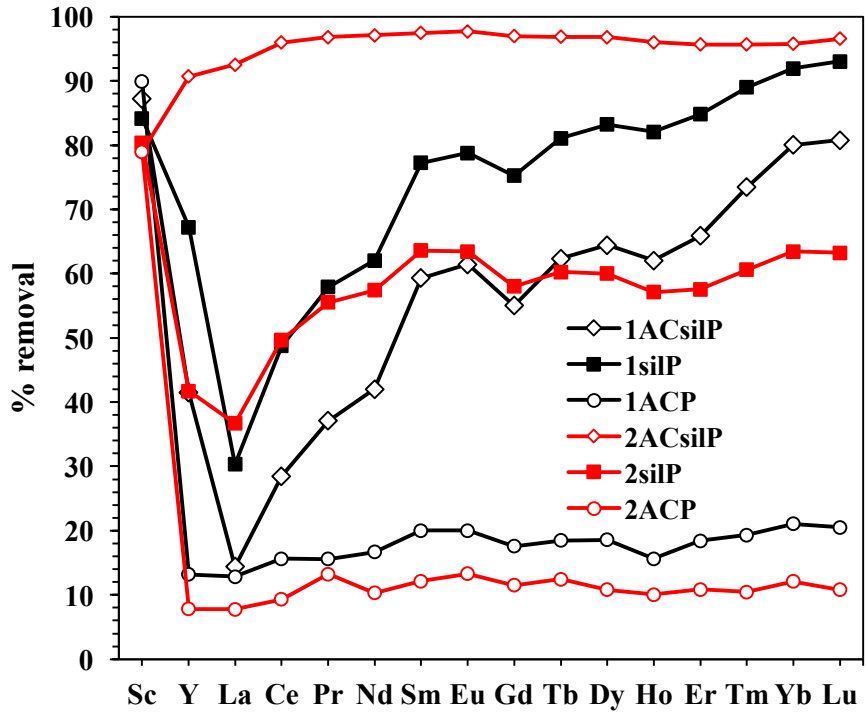

Figure 17. Comparison of PAN-modified, APTES-functionalized activated carbon- and nanosilica-based materials on adsorption of the whole REE-series. pH 5, C_{REE}=5 ppm each, room temperature, t =1 h.

Figure 17 states clearly that nanosilica-APTES component is essential for successful REE adsorption. Adsorption with non-silica adsorbents, 1ACP and 2ACP, was insignificant compared to hybrid- and nanosilica-adsorbents, therefore these adsorbents were excluded from further studies. Solvent evaporation method was drastically more efficient for hybrid adsorbent whereas pure nanosilica was more successful with Method I modification. 2ACsilP outperformed other adsorbents in terms of REE adsorption efficiency at room temperature. However, 1ACsilP, 1silP, and 2silP established higher removal efficiencies with an increase in temperature.

6.4 Real mine water experiments

Feasibility of all hybrid adsorbents for real water applications was studied using real AMD-spiked with REEs. 5 ppm of each REE was added to AMD solution, after which the pH was set

at the desired level. Initial pH of AMD solution before adding REEs was close to 2. Two different AMD solutions were used, first one was collected from the depth of 720 m and the second one from the depth of 500 m. Most experiments were executed with 720 m AMD while 500 m AMD was used to make difference between the best performing adsorbents. After adjusting the pH and REE concentration of AMD solution, the solution was filtered using bottle top filtration unit from VWR with a pore size of 0.45 µm to remove any sludge from precipitation of metals. The initial concentrations of adjusted AMD samples are presented in **Table X**. The pH 5 was selected as an optimum pH for a comparison as it gave significantly higher adsorption efficiencies compared to lower pHs for all studied adsorbents. Higher pH regime should be avoided as mine water is naturally acidic and therefore process would consume higher amounts of chemicals for optimization of the pH. Moreover, hydrolysis of REEs occurs above pH 6. This could also steer adsorption phenomena to the undesired direction (Ramasamy et al., 2017e).

Table X. Concentrations of competing ions in pH-adjusted AMD samples from depths of 720 m and 500 m after addition of REEs (Ramasamy et al., 2017b).

Elements	Concentration [ppm]			
	720 m		500 m	
	pH 2	pH 5	pH 2	pH 5
Al	304.74	283	302.1	272
Cd	0.2	0.14	2.92	2.18
Co	0.3	0.25	1.28	1.25
Cr	0.08	0.01	0.26	0.01
Cu	6.03	1.03	93.5	18.95
Fe	201.41	0.02	300.08	0.04
Mg	49.38	47.71	53.04	50.3
Mn	34.98	27.01	81.45	64.15
Ni	0.38	0.26	2.34	1.72
S	1,597.82	1,412.56	2,300.08	2,072.94
Si	55.96	22.69	67.75	14.36
Zn	85.38	75.71	117.9	107.5

Studied AMD-solutions contained very high amounts of trivalent competing ions such as Fe and Al, which could have a huge impact on the performance of studied adsorbents. Sc precipitated along with Fe during the pH adjusting procedure and therefore adsorption of only 15 REEs was compared from AMD. Even if the Fe particles are precipitated from solution at higher pH regime, Al concentration is in different magnitude comparing to REEs. Particularly, the presence

of Al^{3+} ions caused problems with selective Sc^{3+}-separation with modified silica gels (*5 Application I: Selective separation of scandium*).

6.4.1 Type I: silica-chitosan hybrid gel beads

Group II adsorbents were utilized to study the significance of ligand modification as they gave best results on REE series adsorption. Benefits of PAN-modification can be observed when comparing adsorption rates of competing ions on adjusted AMD. Ligand-modified adsorbents generally adsorbed considerably smaller amount of manganese and copper from the solution whereas the efficiency for both adsorbents was great. Despite PAN-modified beads had higher efficiency compared to AcAc-modified beads, the latter ones resulted in drastically higher selectivity as they removed less than 10 % of competing ions. Differences between ligand modified and unmodified adsorbents in the removal of competing ions from AMD are presented in **Figure 18**.

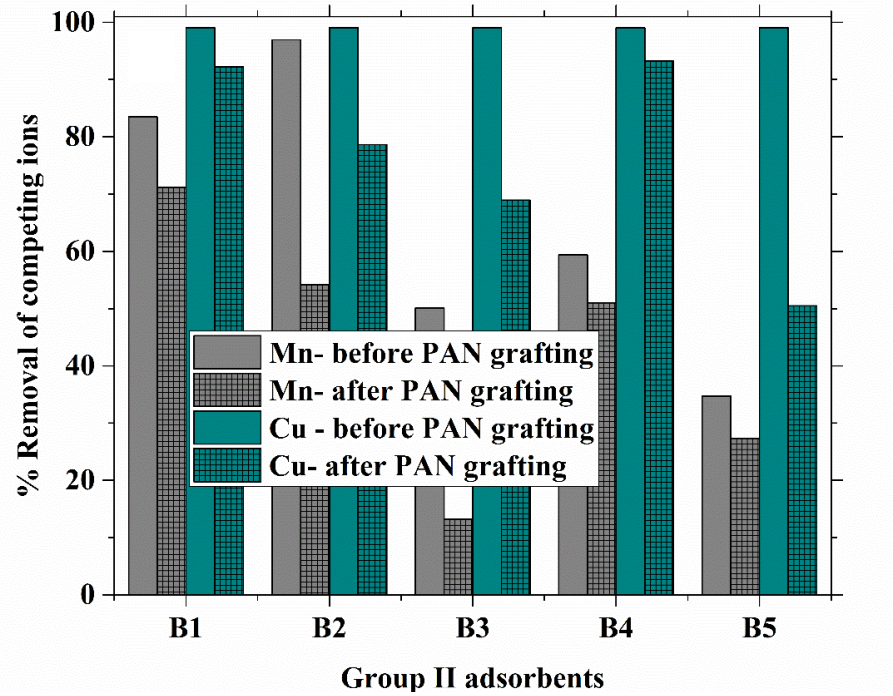

Figure 18. Effect of ligand grafting on adsorption of competing ions in REE recovery from AMD with functionalized silica-chitosan hybrid gel beads. pH 5, C_{REE}=5 ppm each, T=45 °C, t =1 h (Ramasamy et al., 2017b).

The effect of silanization was emphasized in terms of selectivity in AMD experiments. Beads without silane-functionalization established similar adsorption capacities compared to the functionalized ones but distinct differences in affinity towards competing ions were observed (**Figure 19**). APTES- and MTM-functionalized beads established lower affinities towards competing ions in most cases, especially with C1-based modifications. AcAc-modified beads showed minimal adsorption towards competing ions from AMD solutions. Even if the maximum capacities were considerably lower compared to PAN-modified beads, selectivity towards REEs over other ions was superior.

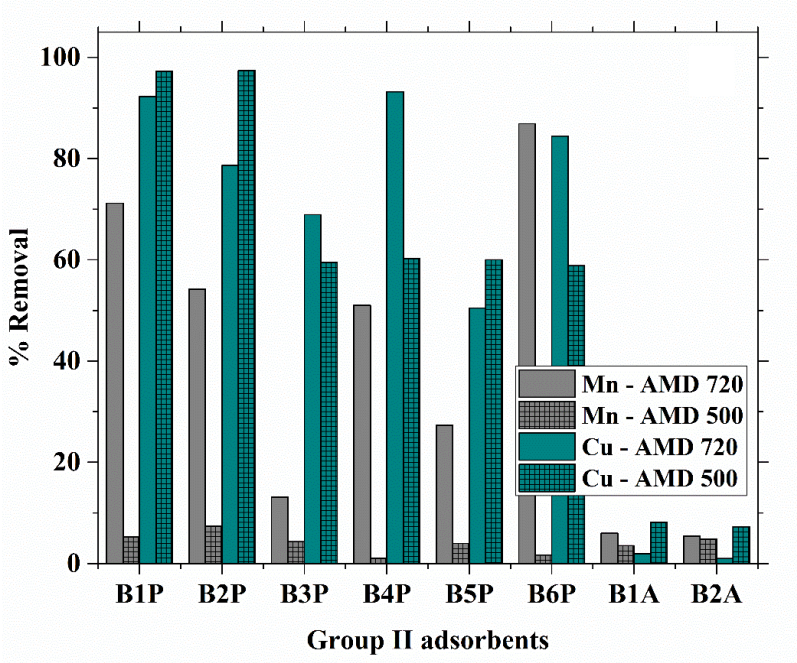

Figure 19. Effect of silanization and ligand modification on the selectivity of group II silica-chitosan hybrid gel beads towards competing ions. pH 5, C_{REE}=5 ppm each, T=45 °C, t =1 h. (Ramasamy et al., 2017b).

Figure 20 concludes the removal percentages of 16 REES with the best PAN- and AcAc-modified adsorbents from each preparation method. REE-enhanced sample from a depth of 720 m was used at pH 5 for comparison of these adsorbents. Based on these results, method II is recommendable for bead preparation, as group II beads showed the best efficiency among all the beads followed by group I and finally by group III. At pH 2, none of the beads showed desirable adsorption from AMD, but with an increase in pH, at the value of 5, B6P achieved

nearly complete adsorption of REEs. Similar to prior results with whole REE series demonstrated in Ramasamy *et al.*, preference towards LREE or HREE is clearly pH dependent (Ramasamy et al., 2017c). At pH 5, most adsorbents had a higher affinity towards HREEs. Furthermore, ionic radii could affect greatly on affinities. According to **Figure 20**, REE adsorption increased considerably with decreasing ionic radii. Y^{3+} follows this pattern as well, even though it behaves differently compared to lanthanides, as its ionic radius is closest to Ho^{3+} among all the REEs. (Ramasamy et al., 2017c).

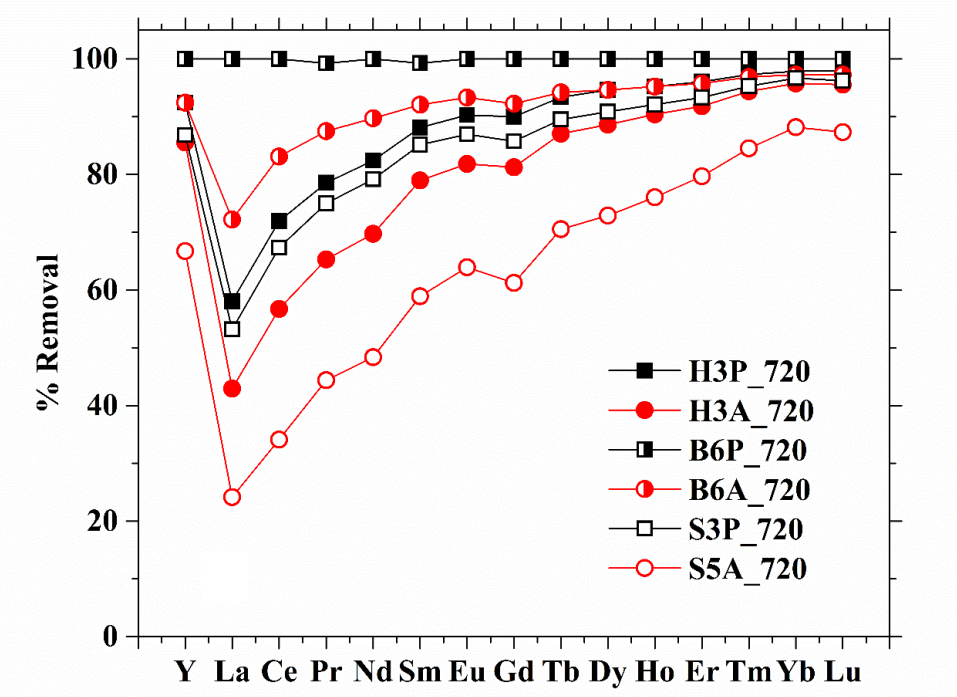

Figure 20. Adsorption of REEs from AMD (720 m) with the best PAN- and AcAc-modified silica-chitosan hybrid gel bead adsorbents of different preparation methods. pH 5, C_{REE}=5 ppm each, T=45 °C, t =1 h (Ramasamy et al., 2017b).

Figure 21 represents a comparison of silanized group II adsorbents in REE removal from AMD samples taken from a depth of 500 m at pH 5. The concentration of competing ions was considerably higher which lowered the REE-removal efficiency of adsorbents. However, distinct differences can be observed between MTM- and APTES-modified beads on the behalf of MTM-

silanized beads. This is in contrary to results with silica gels, where APTES-modifications established considerably higher adsorption capacities. Higher affinity towards HREEs was observed also with PAN-modified adsorbents.

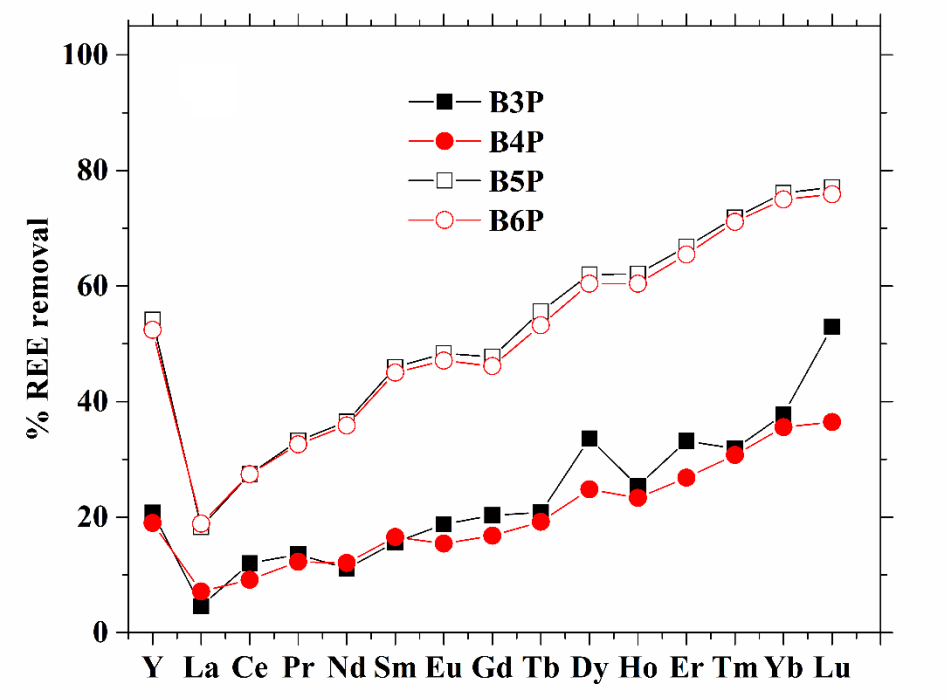

Figure 21. Comparison of PAN-modified, APTES- (3&4) or MTM-silanized (5&6) silica-chitosan hybrid gel beads on adsorption of REEs from AMD (500 m). pH 5, C_{REE}=5 ppm each, T=45 °C, t =1 h. (Ramasamy et al., 2017b).

6.4.2 Type II: carbon nanotube -nanosilica composites

All hybrid adsorbents from type II were selected for AMD experiments. Results are presented in **Figure 22.** From studied adsorbents, 2MWNTsilP established superior results among all CNT-based adsorbents with removal efficiency for most REEs between 60 and 80 % whereas La^{3+}-removal stayed just above 40 %. Among other adsorbents SWNTsil offered the highest capacity, closely followed by 1SWNTsilP and 1MWNTsilP. For all adsorbents, a slight increase in adsorption was observed towards HREEs as expected at pH 5. However, adsorption of Yb^{3+} and Lu^{3+} dropped for all adsorbents increasingly for those with lower adsorption capacities. The least efficient adsorbents MWNTsil and 1MWNTsilP showed negligible adsorption for Yb^{3+} and Lu^{3+}, while removal of other REEs was between 10 and 35 %. These results emphasize the

significance of preparation method, especially for MWNT-adsorbents. MWNT possesses great potential as support material for chelating agents if the modification is executed with right methods.

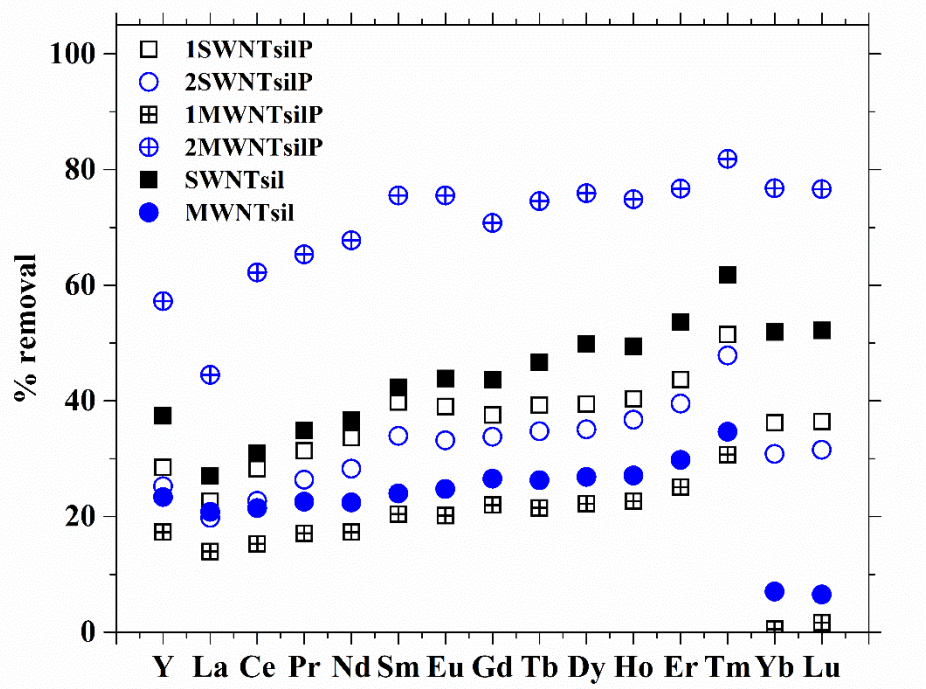

Figure 22. Adsorption of rare earth elements from AMD with PAN-modified, APTES-functionalized CNT- and nanosilica-based adsorbents. pH 5, C_{REE}=5 ppm each, T=45 °C, t =1 h.

6.4.3 Type III: activated carbon -nanosilica composites

Capability for REE recovery from AMD was studied in a similar manner as for other adsorbents in this study. 720 m AMD was utilized at pH 5 for adsorption experiments at room temperature and at 45 °C. In AMD-experiments, adsorption capacity for REEs increased with increasing temperature also for 2ACsilP, despite earlier results from temperature studies with the whole REE-series. Results from experiments 45 °C are presented in **Figure 23**.

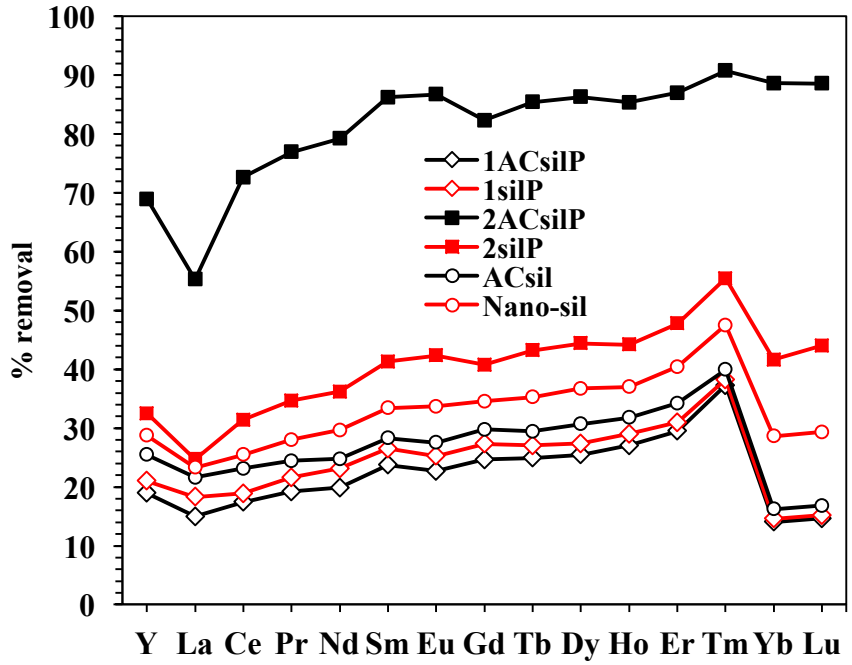

Figure 23. Comparison of PAN-modified, APTES-functionalized activated carbon- and nanosilica-based adsorbents on the recovery of rare earth elements from AMD containing the whole REE series. pH 5, C_{REE}=5 ppm each, T=45 °C, t =1 h.

2ACsilP established superior REE recovery compared to other materials. These results emphasize the significance of ligand modification, especially regarding the method of ligand modification. Type III -adsorbents can be listed in order by preparation method based their REE removal efficiency: group II > group III > group I. Solvent evaporation method proved to be a superior method for ligand modification as adsorbents prepared by other performed worse than unmodified adsorbents. A drop of adsorption capacity was observed for Yb^{3+} and Lu^{3+} with adsorbents possessing lower adsorption capacities. Similar behavior was noticed for CNT-based adsorbents. As strong affinities towards HREEs were not observed from AMD compared to the whole REE-series.

6.5 Characterization

FTIR spectra were analyzed from best adsorbents before and after adsorption to investigate the presence of surface modifications in hybrid adsorbents and to obtain further understanding of adsorption mechanisms. FTIR spectra are presented in **Figure 24** (type I- chitosan-silica beads),

Figure 25 (type II- CNT-nanosilica composites), and **Figure 26** (type III- AC-nanosilica composites). Si – O vibrations can be seen in all FTIR spectra at around 450 (bending vibration), 800 (stretching vibration), 1070 cm^{-1}(asymmetric vibration) (Kaur and Gupta, 2008; Kulkarni et al., 2008; Ramasamy et al., 2017e). Strong band above 1400 cm^{-1} in **Figure 24** could be from the vibrations of -OH groups of chitosan (Sionkowska et al., 2004) whereas small bands at 2850 cm^{-1} represent symmetric C – H stretching (Kulkarni et al., 2008). Presence of bands at 1400 cm^{-1} for also CNT- and AC-adsorbents refers to the presence of OH via PAN or other surface functional groups from the manufacturing process (Henning and von Kienle, 2010; Rao et al., 2007; Sionkowska et al., 2004). The bands at 700, 1500, 1540, and 1590 cm^{-1} are due to stretching vibration of C = C bonds in benzenoid- and pyridyl-units of PAN (Kaur and Gupta, 2008). C – N stretching vibration of PAN-, APTES-, and chitosan moieties appears around 1300 cm^{-1} (Kaur and Gupta, 2008). These bands can be observed in all spectra which states the presence of the ligand modification on the surface of the hybrid adsorbents. According to Ţucureanu *et al*., pure CNT doesn't give significant FTIR signals, but aforementioned C = C stretching vibration bonds could also refer to carbon backbone of CNT and AC (Ţucureanu et al., 2016).

Disappearance or major decrease in bands between 1300 and 1500 cm^{-1} was noticed for all adsorbents. This refers that adsorption has occurred on sites including amino groups of PAN- and APTES-moieties. Based these results, the amino groups and hydroxyl groups in chitosan of type I -adsorbents have also been involved in the adsorption process. Moreover, this also refers on adsorption to carbon structures of type II and III -adsorbents. Increased bands around 1700 cm^{-1} for silica-chitosan beads could be due to water adsorption (Kulkarni et al., 2008).

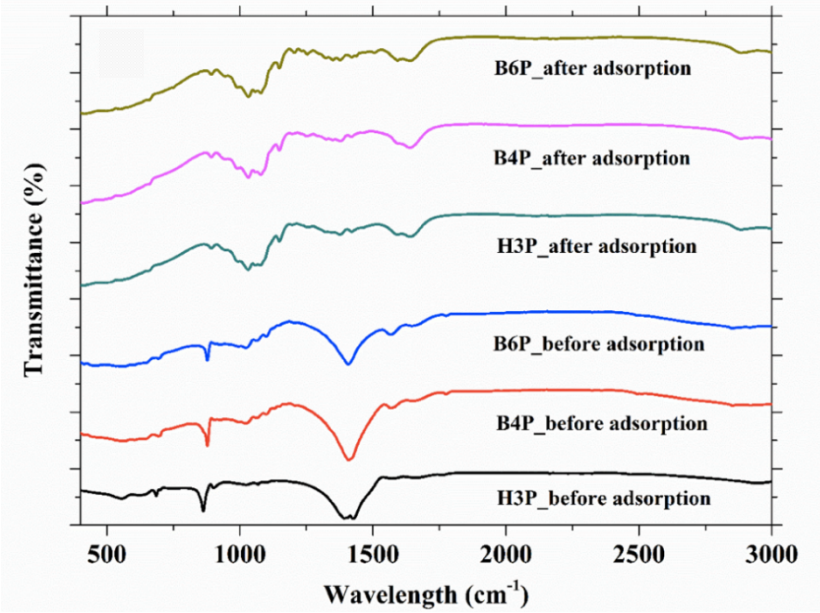

Figure 24. FTIR spectra of PAN-modified, APTES- (4) or MTM-functionalized (3&6) silica-chitosan hybrid gel beads before and after adsorption of rare earth elements from acid mine drainage pH 5, C_{REE}=5 ppm each, T=45 °C, t=1 h. (Ramasamy et al., 2017b).

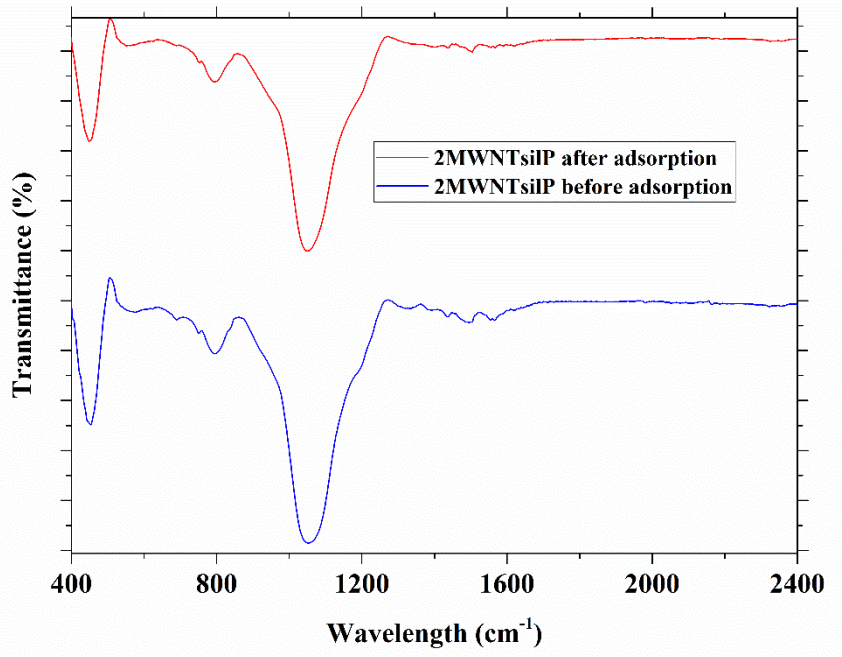

Figure 25. FTIR spectra of PAN-modified, APTES-functionalized MWNT-nanosilica hybrid adsorbent before and after adsorption of rare earth elements from acid mine drainage. pH 5, C_{REE}=5 ppm each, T=45 °C, t=1 h.

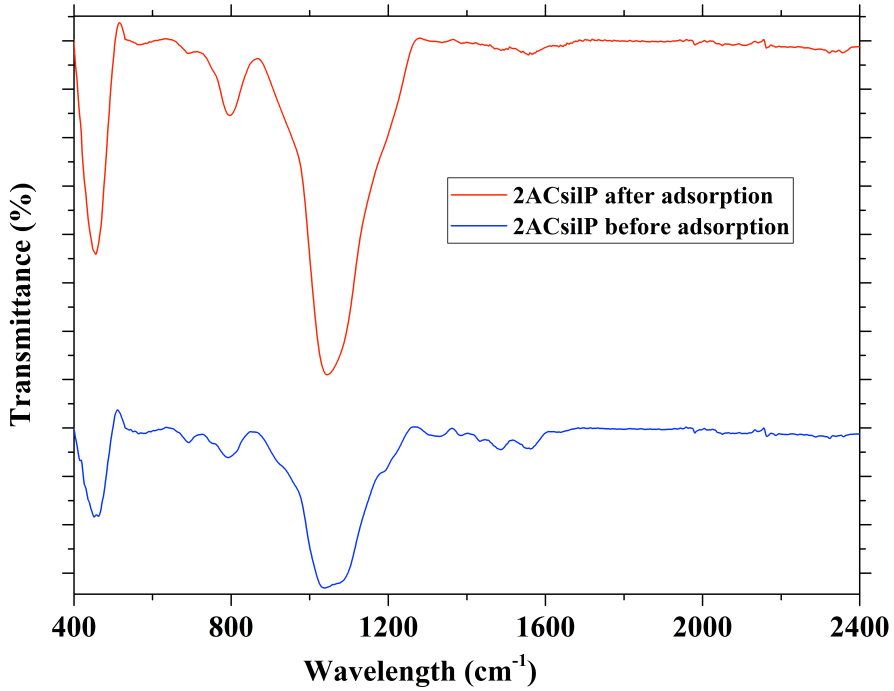

Figure 26. FTIR spectra of PAN-modified, APTES-functionalized AC-nanosilica hybrid adsorbent before and after adsorption of rare earth elements from acid mine drainage. pH 5, C_{REE}=5 ppm each, T=45 °C, t=1 h.

Zeta potential measurements were executed for silica-chitosan hybrid gel beads to investigate the charge of adsorbents at different pH levels. Beads were crushed and mixed with water corresponding to adsorption experiments (5 mg:5 ml). After this, the pH of solutions was set at the desired level. Results from zeta potential measurements (**Figure 27**) indicate that all the beads have positive surface zeta potential at acidic pH regime. Isoelectric point for studied adsorbents does not fall into pH regime applied in this study as higher pH is required for neutral zeta potential values for these adsorbents. This indicates adsorbents are at protonated state at studied pH regime. Therefore, protonation of nitrogen atoms in chitosan-, APTES-, and PAN-structures could play important role in adsorption of REEs.

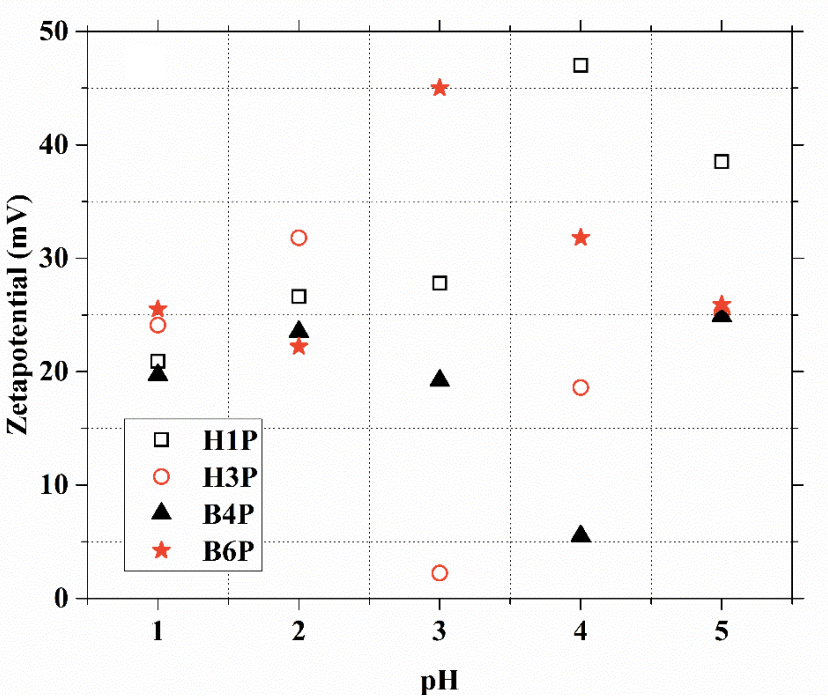

Figure 27. Effect of pH on the zeta potential of silica-chitosan hybrid gel beads (Ramasamy et al., 2017b).

6.6 Comparison

6.6.1 Adsorption capacities

Performance of all adsorbents used over the course of study was compared in order to clarify the differences between performances of each adsorbent group. Single component systems with Sc^{3+}, La^{3+}, and Y^{3+} were compared in terms of adsorption capacities and optimal adsorption times. Maximum capacities of adsorbents from type II and III along with the best fitting isotherm model amongst the studied three isotherms are presented in **Table XI**. Results from Sc^{3+} adsorption for type II are excluded due to negligible adsorption at high concentration which resulted in a poor fit on given isotherms.

Table XI. Adsorption capacities of the best novel hybrid adsorbents from each group on adsorption of Sc^{3+}, La^{3+}, and Y^{3+} from single component systems. pH 5, room temperature, t=24 h.

Adsorbent	Adsorption capacity [mg/g]			Isotherm model
	Sc^{3+}	La^{3+}	Y^{3+}	
Group II Beads	>200	>200	>200	-
2MWsilP	-	106.61	79.75	Langmuir
r^2		0.87	0.56	
2ACsilP	80.28	195.10	112.32	Freundlich
r^2	0.97	0.87	0.96	
2silP	83.52	170.18	106.05	Freundlich
r^2	0.93	0.83	0.96	

Exact adsorption capacities for silica-chitosan hybrid gel beads were not determined due to high adsorption capacity. Beads were capable to remove 99.99 % of adsorbate even at the highest studied concentrations, predicted to be around or more than 200 mg/g. Among the other adsorbents, type III -materials had highest efficiencies in single component systems. 2ACsilP established highest capacities in its group. Adsorption isotherms of type III -adsorbents followed Freundlich isotherm which refers heterogeneous multilayer adsorption (Dada, A. et al., 2012). CNT-based showed negligible adsorption of Sc^{3+} in higher concentrations which led to poor fit with studied isotherm models. For La^{3+} and Y^{3+}, the most CNT-materials followed Langmuir isotherm which refers to monolayer adsorption. Isotherm parameters for these adsorbents are presented in **Table XII**.

Table XII. Isotherm parameters for the adsorption of Sc^{3+}, La^{3+}, and Y^{3+} from single component systems with the best carbon- and nanosilica-based adsorbents used in this study.

Ion	2MWsilP Langmuir		2ACsilP Freundlich		2SilP Freundlich	
	q_m	K_L	K_f	n_f	K_f	n_f
Sc^{3+}	-	-	9.91	2.15	10.95	2.19
La^{3+}	106.61	29.46	54.99	3.50	36.18	2.97
Y^{3+}	79.75	19.44	32.99	3.61	38.62	4.49

Freundlich heterogeneity factor was $n_f > 1$ for all ions which refers to normal (non-cooperative) adsorption. While $1 < n_f < 10$ refers to favorable adsorption. Relatively low $1/n_f$ -values state that adsorption is heterogeneous. (Dada, A. et al., 2012). Since B6P beads established nearly 100 % adsorption for all REEs from AMD and intraseries, their efficiency was further studied with REE-solutions at higher concentrations. Nonlinear least squares regression was used to fit Langmuir, Freundlich, and Sips equations for each REE separately. Adsorption capacities determined with Freundlich equations separately for each element are presented in **Table XIII**, as they gave the best fit among studied isotherms.

Table XIII. Adsorption capacities of PAN-modified, MTM-functionalized silica chitosan hybrid gel beads (B6P) towards 16 rare earth elements in a multicomponent system based on Freundlich isotherm model. pH 5, T=45 °C, t=1 h.

	Adsorption capacity			
Ion	**mg/g**	**mmol/g**	**r^2**	**n_f**
Sc^{3+}	10.21	0.227	0.78	0.68
La^{3+}	8.66	0.097	0.84	0.24
Ce^{3+}	8.28	0.060	0.84	0.28
Pr^{3+}	10.42	0.074	0.87	0.32
Nd^{3+}	9.27	0.066	0.86	0.36
Sm^{3+}	11.84	0.082	0.89	0.35
Eu^{3+}	9.39	0.062	0.85	0.39
Gd^{3+}	10.36	0.068	0.87	0.37
Tb^{3+}	10.05	0.064	0.87	0.33
Y^{3+}	8.51	0.054	0.79	0.35
Dy^{3+}	8.81	0.054	0.85	0.33
Ho^{3+}	9.13	0.055	0.85	0.31
Er^{3+}	8.73	0.052	0.85	0.31
Tm^{3+}	12.19	0.072	0.85	0.33
Yb^{3+}	8.89	0.051	0.83	0.31
Lu^{3+}	8.95	0.051	0.84	0.30
Total q	**153.69**	**1.191**		

B6P beads established total adsorption capacity of over 150 mg/g for all the REEs. Higher adsorption towards certain REEs presented in **Table XIII** is in line with slightly higher initial concentrations, significant differences towards any specific REE were not observed in these conditions. Adsorption of Sc^{3+} ions was significantly higher based on molarity, but since the solutions were prepared based on mass-concentrations (mg/L), the initial molar concentration

of Sc was higher. As Freundlich isotherm resulted in the best fit, it can be assumed that adsorption is heterogeneous and occurs on multiple layers. Based on values of Freundlich heterogeneity factors, REE adsorption with hybrid beads was cooperative (Dada, A. et al., 2012). Required times for reaching adsorption equilibrium in single component systems are presented in **Table XIV**.

Table XIV. Comparison adsorption equilibrium times for adsorption of Sc^{3+}, La^{3+}, and Y^{3+} with PAN-modified, APTES-functionalized CNT- and AC-nanosilica hybrid adsorbents. pH 4, Ci=25 ppm, room temperature.

Type	Adsorbent	Sc	La	Y
I	Group II beads	<5 min	<5 min	<5 min
II	2MWsilP	24 h	<15 min	<15 min
III	2ACsilP	24 h	<15 min	<30 min
	2silP	8 h	<30 min	2 h

Silica-chitosan beads showed superior performance in terms of single component adsorption. Adsorption was rapid towards all studied REEs and nearly complete adsorption was achieved under five minutes. For other adsorbents, adsorption of La^{3+} and Y^{3+} was significantly faster compared to Sc^{3+}. Generally, the trend in adsorption kinetics was: Type I > Type II > Type III from fastest to slowest. Differences can be seen especially in Sc^{3+} adsorption. For other studied ions, adsorption was relatively fast with all adsorbents.

6.6.2 REE recovery from AMD

The best performing adsorbents from each group were compared based on the performance in the main objective of this study, REE separation from AMD. The experiments were conducted at pH 5, 45 °C temperature and 1 hour contact time. The results are presented in **Figure 28**.

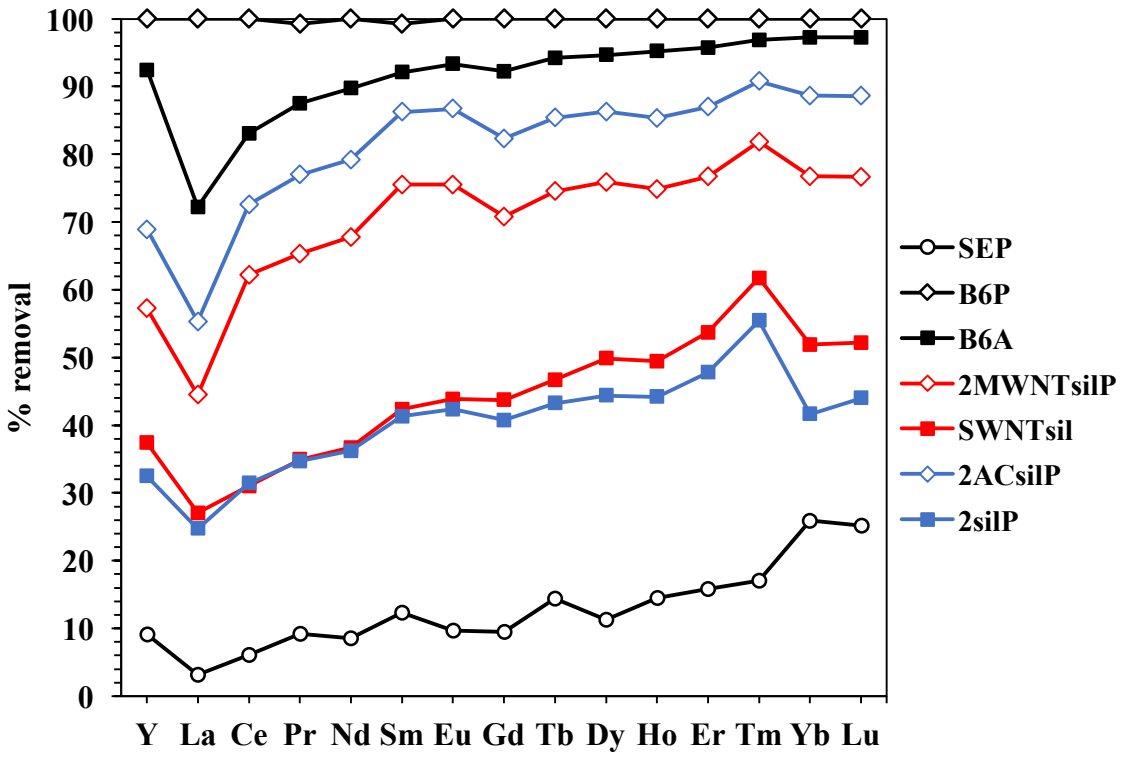

Figure 28. Comparison of REE removal on AMD (720 m) with the best novel hybrid adsorbents from each application and type. pH 5, C_{REE}=5 ppm each, T=45 °C, t=1 h.

Silica-chitosan hybrid gel beads established superior REE adsorption among all adsorbents investigated over the course of this study. Especially in the case of PAN-modified beads, as they established almost 100 % REE recovery even from 10 ppm concentrations. Non-hybrid silica gel adsorbents showed rather poor performance for real mine water application. Nanosilica-adsorbent with similar modification established significantly higher REE-removal efficiency from AMD compared to its silica gel -based counterpart. Solvent evaporation method resulted in the most efficient adsorbents amongst all studied methods for every type of adsorbents. Silica-chitosan beads, MWNT-nanosilica, AC-nanosilica, and nanosilica -based adsorbents all established higher REE recovery with aforementioned preparation method. This could be due to a higher amount of PAN on the adsorbent surface as in another method PAN-moieties could be trapped inside the beads or washed away with the solution during the rinsing process.

6.6.3 Adsorption mechanism

Adsorption of REEs on silica-chitosan beads could occur as Guibal *et al*. stated in their study: REE adsorption at lower pH regime occurs via ion pair formation due to the protonated state of adsorbent. Ligand coordination with N- and O-groups of PAN and AcAc plays role in adsorption. At higher pH regime, where the unprotonated moieties exist, REE adsorption occurs via coordination through nitrogen and oxygen ligand exchange mechanism and slower ligand exchange resulting from ion pair binding (Guibal et al., 2002). High surface zeta potential values even at pH 5 (≥25 V) indicate that protonated moieties are present over the whole studied pH regime.

FTIR results emphasize the importance of amino groups of PAN and APTES for all adsorbents. Presence of additional amino groups in chitosan moieties for hybrid gel beads could be a significant factor resulting in superior performance over other studied adsorbents. The significance of chitosan moieties is even more important since also OH-groups could take part in adsorption according to FTIR spectra. It is probable that OH-groups of PAN and another surface-functional group are playing a significant role in adsorption with carbon-based materials.

6.6.4 Silicon leaching

Stability and reusability of silica gel -based adsorbents can suffer due to leaching of silicon from adsorbent to solution. This is a common problem with silica gel -based adsorbents (Ramasamy et al., 2017a, 2017c, 2017e). There are multiple mentions in literature stating that stability of silica gel can be increased by modification with specific chelating agents (Airoldi and Alcântara, 1995; Jal, 2004). To study the effect of leaching, silicon concentrations after adsorption process were measured from all solutions. Silicon leaching was observed for all studied adsorbents. However, among the silica-chitosan beads, leaching rates were considerably higher for less efficient adsorbents. As leaching evidently decreases stability and efficiency of adsorbent. 2MWNTsilP showed the lowest leaching rates among the type II -adsorbents prepared using solvent evaporation method. For 2ACsilP however, silicon leaching rates were relatively high compared to other AC-based adsorbents.

6.6.5 REE recovery from adsorbents

H3P, B4P, B6P, and B6A recorded the most competent results among studied silica-chitosan hybrid adsorbents and were therefore selected for preliminary recovery experiments. 2MWsilP and 2ACsilP were selected from type II and III respectively. 1 M nitric acid and 2 M hydrochloric acid were utilized for the experiments. 5 ml of acid was added on the saturated adsorbents after adsorption of REEs from 720 m AMD at pH 5. Solutions were mixed for 5 to 15 minutes at a temperature of 45 °C to recover the REEs from adsorbents. Similar behavior was observed for all studied adsorbents. These conditions resulted in 85 to 95 % recovery of adsorbed REEs from all studied hybrid adsorbents along with the recovery of competing ions, HNO_3 being slightly more efficient compared to HCl. From resulting solution, REEs can be recovered easily due to the significantly smaller amount of competing ions present.

7 Future outlook

These adsorbents, especially PAN-modified, MTM-functionalized silica chitosan hybrid beads possess the great capability of REE removal from mine water. Possible applications could be further studied with red mud leachate along other potential real-life applications as increasing REE demand requires sustainable solutions. MTM-modified silica gels showed promising results in terms of selectivity towards Sc^{3+}, this modification could also be applied on CNT-nanosilica adsorbent to investigate more selective Sc^{3+} removal. Hybrid adsorbents with these modifications were prepared for the first time in this study. It must be noted that the amounts of chemicals used for same ligand modification and silanization were based on previous silica gel experiments (Ramasamy et al., 2017e, 2017a, 2017c). Optimization of these parameters could affect the adsorption process considerably. Different ratios between the backbone materials (silica, chitosan, and carbon) for the most efficient adsorbents should also be examined to optimize the synthesis process. Further attention should be paid on optimization of REE recovery after adsorption process. The best adsorbents in this study, group II silica-chitosan hybrid gel beads, could be utilized for electrode coating or as ion exchange materials in carbon-based capacitive deionization (CDI) or electrodeionization (EDI) system for energy-efficient mine water treatment.

8 Conclusions

The aim of this thesis was to develop, two different applications of selective REE-separation from industrial impurities. Selective scandium recovery from artificial industrial wastewater (Application I) and the recovery of whole REE-series from real AMD (Application II) by novel ligand modified hybrid adsorbents were investigated. Selective scandium separation (Application I) from solutions containing common industrial impurities was studied with just silica gel adsorbents modified with ligands (PAN and AcAc) and silanes (APTES and MTM) in binary- and multi-component systems. According to this assessment, newly developed MTM-modified silica gels established the highest selectivity towards scandium ions whereas APTES-modifications offered superior adsorption capacity showing co-separation of other ions as well. The strategy for selective scandium removal in the presence of other impurities was also developed as a result of this study.

As a part of Application II, the novel hybrid adsorbents for REE recovery from mine water were synthesized and evaluated. Silica-chitosan, carbon nanotube-nanosilica, and activated carbon-nanosilica hybrid adsorbents were assessed for this specific purpose using different methods of adsorbent preparation. Effect of surface modification on REE recovery with and without ligand grafting and silanization was investigated. The results revealed that silanization, ligand grafting, and hybridization proved to enhance the properties of adsorbents in terms of adsorption capacity, selectivity, and stability. REE adsorption process was assessed using single component system, whole REE-series, and real acid mine drainage. PAN-modified silica-chitosan hybrid gel beads showed superior efficiency for REE recovery from AMD compared to other hybrid adsorbents whereas AcAc-modified versions showed highest selectivities towards REEs over competing ions. High REE recovery rates were achieved even at pH 2 in the absence of competing ions. In mine water studies, optimum pH for REE recovery was considerably higher at pH 5 due to the presence of high concentrations of other metal ions. Similarly, PAN- and APTES-modified onto AC-nanosilica and MWNT-nanosilica composites showed the highest recovery of REEs. Overall, solvent evaporation method proved to be the most efficient method of ligand modification for all the adsorbents under consideration. For this application, the best adsorbent was proved to be silica-chitosan hybrid beads, supported by the merits of instant rapid

adsorption and desorption of REEs, which makes them a feasible option for REE recovery applications from mine waters.

References

Ahmed, M.J., Dhedan, S.K., 2012. Equilibrium isotherms and kinetics modeling of methylene blue adsorption on agricultural wastes-based activated carbons. Fluid Phase Equilibria 317, 9–14. doi:10.1016/j.fluid.2011.12.026

Airoldi, C., Alcântara, E.F.C., 1995. Silica-gel-immobilized acetylacetone—some thermodynamic data in non-aqueous solvents. Thermochim. Acta 259, 95–102. doi:10.1016/0040-6031(95)02295-D

Babel, S., 2003. Low-cost adsorbents for heavy metals uptake from contaminated water: a review. J. Hazard. Mater. 97, 219–243. doi:10.1016/S0304-3894(02)00263-7

Bart, H.-J., von Gemmingen, U., 2005. Adsorption, in: Wiley-VCH Verlag GmbH & Co. KGaA (Ed.), Ullmann's Encyclopedia of Industrial Chemistry. Wiley-VCH Verlag GmbH & Co. KGaA, Weinheim, Germany. doi:10.1002/14356007.b03_09.pub2

Binnemans, K., Jones, P.T., Blanpain, B., Van Gerven, T., Yang, Y., Walton, A., Buchert, M., 2013. Recycling of rare earths: a critical review. J. Clean. Prod. 51, 1–22. doi:10.1016/j.jclepro.2012.12.037

Borra, C.R., Pontikes, Y., Binnemans, K., Van Gerven, T., 2015. Leaching of rare earths from bauxite residue (red mud). Miner. Eng. 76, 20–27. doi:10.1016/j.mineng.2015.01.005

Cadek, M., Vostrowsky, O., Hirsch, A., 2010. Carbon, 7. Fullerenes and Carbon Nanomaterials, in: Wiley-VCH Verlag GmbH & Co. KGaA (Ed.), Ullmann's Encyclopedia of Industrial Chemistry. Wiley-VCH Verlag GmbH & Co. KGaA, Weinheim, Germany. doi:10.1002/14356007.n05_n06

Castor, Stephen, Hedrick, James, 2006. Rare Earth Elements, in: Industrial Minerals and Rocks. pp. 769–788.

Chiron, N., Guilet, R., Deydier, E., 2003. Adsorption of Cu(II) and Pb(II) onto a grafted silica: isotherms and kinetic models. Water Res. 37, 3079–3086. doi:10.1016/S0043-1354(03)00156-8

Dada, A., Olalekan, A., Olatunya, A., Dada, O., 2012. Langmuir, Freundlich, Temkin and Dubinin_Radushkevich Isotherms Studies of Equilibrium Sorption of Zn2+ Unto Phosphoric Acid Modified Rice Husk. IOSR J. Appl. Chem. 3, 38–45.

Gao, Y., Lee, K.-H., Oshima, M., Motomizu, S., 2000. Adsorption Behavior of Metal Ions on Cross-linked Chitosan and the Determination of Oxoanions after Pretreatment with a Chitosan Column. Anal. Sci. 16, 1303–1308. doi:10.2116/analsci.16.1303

Guibal, E., 2005. Heterogeneous catalysis on chitosan-based materials: a review. Prog. Polym. Sci. 30, 71–109. doi:10.1016/j.progpolymsci.2004.12.001

Guibal, E., 2004. Interactions of metal ions with chitosan-based sorbents: a review. Sep. Purif. Technol. 38, 43–74. doi:10.1016/j.seppur.2003.10.004

Guibal, E., Von Offenberg Sweeney, N., Vincent, T., Tobin, J.., 2002. Sulfur derivatives of chitosan for palladium sorption. React. Funct. Polym. 50, 149–163. doi:10.1016/S1381-5148(01)00110-9

Henning, K.-D., von Kienle, H., 2010. Carbon, 5. Activated Carbon, in: Wiley-VCH Verlag GmbH & Co. KGaA (Ed.), Ullmann's Encyclopedia of Industrial Chemistry. Wiley-VCH Verlag GmbH & Co. KGaA, Weinheim, Germany. doi:10.1002/14356007.n05_n04

Hirano, S., 2002. Chitin and Chitosan, in: Wiley-VCH Verlag GmbH & Co. KGaA (Ed.), Ullmann's Encyclopedia of Industrial Chemistry. Wiley-VCH Verlag GmbH & Co. KGaA, Weinheim, Germany. doi:10.1002/14356007.a06_231

Hokkanen, S., Repo, E., Suopajärvi, T., Liimatainen, H., Niinimaa, J., Sillanpää, M., 2014. Adsorption of Ni(II), Cu(II) and Cd(II) from aqueous solutions by amino modified nanostructured microfibrillated cellulose. Cellulose 21, 1471–1487. doi:10.1007/s10570-014-0240-4

Iakovleva, E., Sillanpää, M., 2013. The use of low-cost adsorbents for wastewater purification in mining industries. Environ. Sci. Pollut. Res. 20, 7878–7899. doi:10.1007/s11356-013-1546-8

Iftekhar, S., Srivastava, V., Sillanpää, M., 2017a. Synthesis and application of LDH intercalated cellulose nanocomposite for separation of rare earth elements (REEs). Chem. Eng. J. 309, 130–139. doi:10.1016/j.cej.2016.10.028

Iftekhar, S., Srivastava, V., Sillanpää, M., 2017b. Enrichment of lanthanides in aqueous system by cellulose based silica nanocomposite. Chem. Eng. J. 320, 151–159. doi:10.1016/j.cej.2017.03.051

Ihsanullah, Abbas, A., Al-Amer, A.M., Laoui, T., Al-Marri, M.J., Nasser, M.S., Khraisheh, M., Atieh, M.A., 2016. Heavy metal removal from aqueous solution by advanced carbon nanotubes: Critical review of adsorption applications. Sep. Purif. Technol. 157, 141–161. doi:10.1016/j.seppur.2015.11.039

Jal, P., 2004. Chemical modification of silica surface by immobilization of functional groups for extractive concentration of metal ions. Talanta 62, 1005–1028. doi:10.1016/j.talanta.2003.10.028

Kaur, A., Gupta, U., 2008. A Preconcentration Procedure Using 1-(2-Pyridylazo)-2-napthol Anchored to Silica Nanoparticle for the Analysis of Cadmium in Different Samples. E-J. Chem. 5, 930–939. doi:10.1155/2008/431916

Khalid, P., Suman, V., Hussain, M., Arun, A., 2015. Toxicology of Carbon Nanotubes - A Review. J. Environ. Nanotechnol. 4, 62–75. doi:10.13074/jent.2015.12.154176

Kimball, S., 2017. Mineral Commodity Summaries 2017.

Kinniburgh, D.G., 1986. General purpose adsorption isotherms. Environ. Sci. Technol. 20, 895–904. doi:10.1021/es00151a008

Kulkarni, S.A., Ogale, S.B., Vijayamohanan, K.P., 2008. Tuning the hydrophobic properties of silica particles by surface silanization using mixed self-assembled monolayers. J. Colloid Interface Sci. 318, 372–379. doi:10.1016/j.jcis.2007.11.012

Kumar, K., 2006. Comparative analysis of linear and non-linear method of estimating the sorption isotherm parameters for malachite green onto activated carbon. J. Hazard. Mater. 136, 197–202. doi:10.1016/j.jhazmat.2005.09.018

Liu, S., 2015. Cooperative adsorption on solid surfaces. J. Colloid Interface Sci. 450, 224–238. doi:10.1016/j.jcis.2015.03.013

Long, K, Van Gosen, B, Foley, N, Cordier, D, 2010. The Principal Rare Earth Deposits of the United States – A Summary of Domestic Deposits and a Global Perspective (No. 2010–5220), Scientific Investigations Report. U.S. Geological Survey, Reston, Virginia.

Machacek, E., Kalvig, P., 2016. Assessing advanced rare earth element-bearing deposits for industrial demand in the EU. Resour. Policy 49, 186–203. doi:10.1016/j.resourpol.2016.05.004

Mahmoud, M.E., Al-Bishri, H.M., 2011. Supported hydrophobic ionic liquid on nano-silica for adsorption of lead. Chem. Eng. J. 166, 157–167. doi:10.1016/j.cej.2010.10.046

McCabe, W., Smith, J., Harriott, P., 1993. Unit Operations of Chemical Engineering, 5th Edition. ed, Chemical and Petroleum Engineering Series. McGraw-Hill Inc.

McGill, I., 2000. Rare Earth Elements, in: Ullmann's Encyclopedia of Industrial Chemistry. Wiley-VCH Verlag GmbH & Co. KGaA.

Mineralprices.com - The Global Source for Metals Pricing [WWW Document], 2017. URL http://mineralprices.com/ (accessed 9.6.17).

Ramasamy, Khan, S., Repo, E., Sillanpää, M., 2017a. Synthesis of mesoporous and microporous amine and non-amine functionalized silica gels for the application of rare earth elements (REE) recovery from the waste water-understanding the role of pH, temperature, calcination and mechanism in Light REE and Heavy REE separation. Chem. Eng. J. 322, 56–65. doi:10.1016/j.cej.2017.03.152

Ramasamy, Puhakka, V., Iftekhar, S., Wojtuś, A., Repo, E., Ben Hammouda, S., Iakovleva, E., Sillanpää, M., 2017b. N- and O- ligand doped mesoperous silica-chitosan hybrid beads

for the efficient, sustainable and selective recovery of rare earth elements (REE) from Acid Mine Drainage (AMD): Understandingthe significance of physical modification and conditioning oh the polymer Environmental Science and Technology (Under Peer Review).

Ramasamy, Puhakka, V., Repo, E., Khan, S., Sillanpää, M., 2017c. Coordination and silica surface chemistry of lanthanides (III), scandium (III) and yttrium (III) sorption on 1-(2-pyridylazo)-2-napththol (PAN) and acetylacetone (acac) immobilized gels. Chem. Eng. J. 324, 104–112. doi:10.1016/j.cej.2017.05.025

Ramasamy, Puhakka, V., Repo, E., Sillanpää, M., 2017d. Selective separation of Scandium from Iron, Aluminum and Gold rich waste waterusing various amino and non-amino functionalized silica gels - a comparitive study. J. Clean. Prod. In Press. Accepted manuscript.

Ramasamy, Repo, E., Srivastava, V., Sillanpää, M., 2017e. Chemically immobilized and physically adsorbed PAN/acetylacetone modified mesoporous silica for the recovery of rare earth elements from the waste water-comparative and optimization study. Water Res. 114, 264–276. doi:10.1016/j.watres.2017.02.045

Ramasamy, Wojtuś, A., Repo, E., Kalliola, S., Srivastava, V., Sillanpää, M., 2017f. Ligand immobilized novel hybrid adsorbents for rare earth elements (REE) removal from waste water: Assessing the feasibility of using APTES functionalized silica in the hybridization process with chitosan. Chem. Eng. J. 330, 1370–1379. doi:10.1016/j.cej.2017.08.098

Rao, G., Lu, C., Su, F., 2007. Sorption of divalent metal ions from aqueous solution by carbon nanotubes: A review. Sep. Purif. Technol. 58, 224–231. doi:10.1016/j.seppur.2006.12.006

Ravi Kumar, M.N.., 2000. A review of chitin and chitosan applications. React. Funct. Polym. 46, 1–27. doi:10.1016/S1381-5148(00)00038-9

Repo, E., 2011. EDTA- and DTPA- Functionalized Silica Gel and Chitosan Adsorbents for the Removal of Heavy Metals from Aqueous Solutions (Thesis for the degree of Doctor of Science (in Technology)). Lappeenranta University of Technology, Lappeenranta.

Repo, E., Kurniawan, T.A., Warchol, J.K., Sillanpää, M.E.T., 2009. Removal of Co(II) and Ni(II) ions from contaminated water using silica gel functionalized with EDTA and/or DTPA as chelating agents. J. Hazard. Mater. 171, 1071–1080. doi:10.1016/j.jhazmat.2009.06.111

Repo, E., Warchoł, J.K., Bhatnagar, A., Sillanpää, M., 2011. Heavy metals adsorption by novel EDTA-modified chitosan–silica hybrid materials. J. Colloid Interface Sci. 358, 261–267. doi:10.1016/j.jcis.2011.02.059

Rezvani-Boroujeni, A., Javanbakht, M., Karimi, M., Shahrjerdi, C., Akbari-adergani, B., 2015. Immoblization of Thiol-Functionalized Nanosilica on the Surface of Poly(ether sulfone) Membranes for the Removal of Heavy-Metal Ions from Industrial Wastewater Samples. Ind. Eng. Chem. Res. 54, 502–513. doi:10.1021/ie504106y

Roosen, J., Spooren, J., Binnemans, K., 2014. Adsorption performance of functionalized chitosan–silica hybrid materials toward rare earths. J Mater Chem A 2, 19415–19426. doi:10.1039/C4TA04518A

Roosen, J., Van Roosendael, S., Borra, C.R., Van Gerven, T., Mullens, S., Binnemans, K., 2016. Recovery of scandium from leachates of Greek bauxite residue by adsorption on functionalized chitosan–silica hybrid materials. Green Chem 18, 2005–2013. doi:10.1039/C5GC02225H

Sadovsky, D., Brenner, A., Astrachan, B., Asaf, B., Gonen, R., 2016. Biosorption potential of cerium ions using Spirulina biomass. J. Rare Earths 34, 644–652. doi:10.1016/S1002-0721(16)60074-1

Seco, M., 1989. Acetylacetone: A versatile ligand. J. Chem. Educ. 66, 779. doi:10.1021/ed066p779

Sionkowska, A., Wisniewski, M., Skopinska, J., Kennedy, C.J., Wess, T.J., 2004. Molecular interactions in collagen and chitosan blends. Biomaterials 25, 795–801. doi:10.1016/S0142-9612(03)00595-7

Srivastava, N.C., Eames, I.W., 1998. A review of adsorbents and adsorbates in solid–vapour adsorption heat pump systems. Appl. Therm. Eng. 18, 707–714. doi:10.1016/S1359-4311(97)00106-3

Strosnider, W.H., Nairn, R.W., 2010. Effective passive treatment of high-strength acid mine drainage and raw municipal wastewater in Potosí, Bolivia using simple mutual incubations and limestone. J. Geochem. Explor. 105, 34–42. doi:10.1016/j.gexplo.2010.02.007

Sze, A., Erickson, D., Ren, L., Li, D., 2003. Zeta-potential measurement using the Smoluchowski equation and the slope of the current–time relationship in electroosmotic flow. J. Colloid Interface Sci. 261, 402–410. doi:10.1016/S0021-9797(03)00142-5

Tokalioglu, S., Büyükbas, H., Kartal, S., 2006. Preconcentration of trace elements by using 1-(2-Pyridylazo)-2-naphthol functionalized Amberlite XAD-1180 resin and their determination by FAAS. J. Braz. Chem. Soc. 17, 98–106. doi:10.1590/S0103-50532006000100015

Tong, S., Zhao, S., Zhou, W., Li, R., Jia, Q., 2011. Modification of multi-walled carbon nanotubes with tannic acid for the adsorption of La, Tb and Lu ions. Microchim. Acta 174, 257–264. doi:10.1007/s00604-011-0622-3

Ţucureanu, V., Matei, A., Avram, A.M., 2016. FTIR Spectroscopy for Carbon Family Study. Crit. Rev. Anal. Chem. 46, 502–520. doi:10.1080/10408347.2016.1157013

Uhrlandt, S., 2006. Silica, in: John Wiley & Sons, Inc. (Ed.), Kirk-Othmer Encyclopedia of Chemical Technology. John Wiley & Sons, Inc., Hoboken, NJ, USA. doi:10.1002/0471238961.0914201816012020.a01.pub2

Varma, A.., Deshpande, S.., Kennedy, J.., 2004. Metal complexation by chitosan and its derivatives: a review. Carbohydr. Polym. 55, 77–93. doi:10.1016/j.carbpol.2003.08.005

Wall, F., 2013. Rare earth elements, in: Gunn, G. (Ed.), Critical Metals Handbook. John Wiley & Sons, Oxford, pp. 312–339. doi:10.1002/9781118755341.ch13

Xue, M, 2015. Rare Earth Weekly - Review Feb 25-28.

Zepf, V., 2013. Rare Earth Elements, Springer Theses. Springer Berlin Heidelberg, Berlin, Heidelberg. doi:10.1007/978-3-642-35458-8

Zhang, Lina, Chang, X., Hu, Z., Zhang, Lijun, Shi, J., Gao, R., 2010. Selective solid phase extraction and preconcentration of mercury(II) from environmental and biological samples using nanometer silica functionalized by 2,6-pyridine dicarboxylic acid. Microchim. Acta 168, 79–85. doi:10.1007/s00604-009-0261-0